

**UCLA**

**UCLA Electronic Theses and Dissertations**

**Title**

CTLA4-Ig disrupts muscle fibrosis in the mdx mouse model of Duchenne muscular dystrophy

**Permalink**

<https://escholarship.org/uc/item/4063b538>

**Author**

Kannan, Pranav

**Publication Date**

2021

Peer reviewed|Thesis/dissertation

UNIVERSITY OF CALIFORNIA

Los Angeles

CTLA4-Ig disrupts muscle fibrosis in the *mdx* mouse model of Duchenne muscular dystrophy.

A thesis submitted in partial satisfaction of the requirements for the degree

Master of Science in Physiological Science

by

Pranav Kannan

2021



## ABSTRACT OF THE THESIS

CTLA4-Ig disrupts muscle fibrosis in the *mdx* mouse model of Duchenne muscular dystrophy

by

Pranav Kannan

Master of Science in Physiological Science

University of California, Los Angeles, 2021

Professor James G Tidball, Chair

Despite advancements in our understanding of the immunobiology of Duchenne muscular dystrophy (DMD), previous findings were not translated into improvements in clinical practice. The standard clinical treatment for DMD includes administration of non-specific anti-inflammatory corticosteroids that provide limited benefits for patients and produce non-target effects that impair muscle regeneration. Thus, the search for an efficacious immunotherapy without adverse effects remains imperative. Because DMD pathology is exacerbated by fibrotic mechanisms mediated by myeloid and fibrogenic cells, we examined the effect of an immune suppressing fusion protein consisting of cytotoxic T-lymphocyte-associated protein4 and immunoglobulin G (CTLA4-Ig) in the *mdx* murine model of DMD. We found that CTLA4-Ig ameliorates pathology, via the disruption of fibrotic mechanisms, as treatment reduced collagen accumulation and expression in dystrophic muscle. These findings indicate that CTLA4-Ig treatment has inhibitory effects on profibrotic cells that exacerbate DMD pathology and could potentially serve as a promising treatment option for patients with DMD.

The thesis of Pranav Kannan is approved.

Kenneth Dorshkind

Rachelle H. Crosbie

James G. Tidball, Committee Chair

University of California, Los Angeles

2021

## TABLE OF CONTENTS

I.	Introduction.....	1
II.	Materials and Methods.....	7
III.	Results.....	14
IV.	Discussion.....	19
V.	References.....	41

## LIST OF FIGURES

Figure 1: CTLA4-Ig disrupts costimulation during naïve T-cell activation.....	26
Figure 2: CTLA4-Ig treatment reduces pro-inflammatory macrophage numbers in <i>mdx</i> mice quadriceps muscle.....	27
Figure 3: CTLA4-Ig treatment does not affect anti-inflammatory macrophage numbers in <i>mdx</i> mice quadriceps muscles of intermediate (25 µg/g), and high-dose (50 µg/g) treatment.....	28
Figure 4: CTLA4-Ig treatment reduces pro-fibrotic CD163 <sup>+</sup> macrophage numbers in 4-week old <i>mdx</i> mice.....	29
Figure 5: CTLA4-Ig does not affect collagen accumulation in 4-week old <i>mdx</i> mice .....	30
Figure 6: CTLA4-Ig treatment reduced collagens I and V accumulation in 3-month old <i>mdx</i> mice.....	32
Figure 7: Relative mRNA expression of genes associated with fibrosis in macrophages is not affected by CTLA4-Ig treatment in quadriceps of 4-week and 3-month old <i>mdx</i> mice .....	34
Figure 8: Fibrogenic cells express costimulatory molecules .....	35
Figure 9: HSP47 <sup>+</sup> cells express CTLA-4 binding ligand CD80.....	36
Figure 10: CTLA4-Ig treatment has no effect HSP47 <sup>+</sup> cell numbers in <i>mdx</i> mice.....	37
Figure 11: Relative mRNA expression of fibrotic genes is not affected by CTLA4-Ig treatment in quadriceps of 4-week old <i>mdx</i> mice.....	38
Figure 12: Collagen V relative expression is reduced in quadriceps of CTLA4-Ig treated <i>mdx</i> mice.....	39
Figure 13: Collagen III and fibronectin relative expression is reduced in L929 fibroblasts treated with CTLA4-Ig .....	40

## Introduction

Duchenne muscular dystrophy (DMD) is a lethal, X-linked recessive disorder, that is characterized by progressive muscle degeneration, inflammation, and fibrosis (Jennekens et al. 1991). DMD is caused by mutations in dystrophin, a gene that encodes protein that links the muscle cytoskeleton to the extracellular matrix (ECM) (Hoffman et al. 1987). The absence of functional dystrophin increases susceptibility to contraction-induced injury (Petrof et al. 1993) leading to an influx of immune cells that play major roles in DMD pathology (McDouall et al. 1990).

Leukocyte cell populations contribute significantly to muscle necrosis and fibrosis in the *mdx* mouse model of DMD in which the progression of pathology is represented by an acute phase, regenerative phase, and progressive phase. The acute phase of pathology occurs at 4-weeks of age and is characterized by muscle inflammation and damage (Villalta et al. 2011). Regenerative and progressive phases are characterized by muscle regeneration and fibrosis and are observed in 12-week and 1-year *mdx* mice, respectively (Villalta et al. 2011). Among these leukocyte populations, macrophages dominate inflammatory lesions and can achieve concentrations up to 30,000 cells/mm<sup>3</sup> in dystrophic muscle (Wehling et al. 2001). However, macrophages occur in a spectrum of phenotypes that extend from classically-activated, M1 macrophages to alternatively-activated, M2 macrophages (Mills 2012).

M1 macrophages are pro-inflammatory and peak in the *mdx* model during the acute stage of pathology (Villalta et al. 2011). They are activated by, and secrete pro-inflammatory cytokines, including interferon gamma (IFN $\gamma$ ) (Pace et al. 1983, Philip et al. 1986). M1 macrophages also

contribute to muscle cell lysis via the release of free radicals such as nitric oxide (NO) (Villalta et al. 2009). Macrophage depletions in dystrophic muscle lead to substantial reductions in myofiber damage, indicating that these myeloid populations contribute significantly to muscle damage in dystrophic muscle (Wehling et al. 2001).

Anti-inflammatory M2 macrophages are the predominate leukocyte population in the regenerative and progressive stages of *mdx* pathology. In part, the shift of macrophages to the M2 phenotype in dystrophic muscle is mediated by the anti-inflammatory cytokine IL-10, which deactivates the M1 phenotype (Villalta et al. 2011). M2 macrophages then promote myogenesis and muscle regeneration via the release of factors including Klotho and insulin-like growth factor 1 (IGF-1) (Tonkin et al. 2015, Wehling-Henricks et al. 2018). Despite these beneficial effects, M2 macrophages also increase muscle fibrosis in dystrophic muscle (Wehling-Henricks et al., 2010). This worsens pathology, since excessive accumulation of connective tissue impairs myofiber function leading to perturbations in cardiac and respiratory muscle function. Thus, DMD patients die prematurely by their late 20s following cardiac and/or respiratory failure arising from muscle fibrosis (Ishikawa et al. 2011, Walcher et al. 2011). M2 macrophages contribute to fibrogenesis by providing substrate for collagen synthesis (Wehling-Henricks et al., 2010) and by release of transforming growth factor beta (TGF-beta) (Desguerre et al. 2009, Song et al. 2019). Additionally, M2 macrophages also influence the activity and differentiation of fibro-adipogenic progenitor cells (FAPs) that also increase fibrosis in muscular dystrophy (Lemos et al. 2015). FAPs reside in muscle in a quiescent state, however they are activated by muscle injury, after which they release factors that promote muscle regeneration. FAPs subsequently differentiate into myofibroblasts and promote ECM production and fibrosis

(Contreras et al. 2016). FAP apoptosis is blocked by TGF-beta synthesis (Lemos et al. 2015) thus indicating that M2 macrophages play a critical role in inducing FAP survival and fibrosis.

The adaptive immune system also plays a role in the *mdx* pathology as CD8<sup>+</sup> cytotoxic T-lymphocytes (CTLs), and CD4<sup>+</sup> helper T cells (Spencer et al. 1997, 2001), are present in *mdx* muscles, although at much lower number than macrophages. CTLs are capable of directly killing infected cells following antigen presentation via major histocompatibility complex I (MHC-1) on the surface of antigen presenting cells (APCs) (Hahn et al. 1994). In *mdx* mice, CD8<sup>+</sup> T-cells promote myonuclear apoptosis and necrosis through perforin-mediated cytotoxicity (Spencer et al. 1997). CTL depletions lead to large reductions in apoptotic and necrotic *mdx* muscle tissue (Spencer et al. 1997). CD4<sup>+</sup> T-cells are also a source of several cytokines that influence the differentiation and activation of leukocyte populations that play a role in *mdx* pathology. For example, a subpopulation of helper T-cells known as Th1 cells secrete pro-inflammatory cytokines including IFN $\gamma$ , to activate M1 macrophages and CTLs (Ma et al. 2003, Green et al. 2013). Similar to CD8<sup>+</sup> T-cells, CD4<sup>+</sup> T-cell depletions in *mdx* mice leads to improvements in muscle pathology, while the transfer of *mdx* splenocytes to wild-type, healthy mice increases muscle damage in these recipients (Spencer et al. 2001).

Other subsets of CD4<sup>+</sup> T-cells, including FOXP3<sup>+</sup> T-regs, influence muscle regeneration and play a role in immunoregulation. (Villalta et al. 2014) T-regs are immunosuppressive cells, and they reduce pathology in the *mdx* model (Villalta et al. 2014). Due to their high expression of the anti-inflammatory cytokine, IL-10, concentrations of T-regs are directly correlated with reductions in myofiber damage. (Villalta et al. 2014). The depletion of T-regs in *mdx* muscle increases the

number of inflammatory infiltrates, and IFN $\gamma$  expression, leading to increased proportions of injured myofibers (Villalta et al. 2014). T-regs therefore play a major role in regulating the progression of dystrophic pathology by influencing macrophage activation and suppressing an M1-biased inflammatory response.

Although most of our knowledge of the immunobiology of muscular dystrophy is based on the *mdx* mouse model of DMD, our current understanding of DMD pathology indicates that immunoregulatory interventions may provide new strategies to treat the disease in humans. DMD pathology is progressive, and many of the leukocyte populations that are involved in *mdx* pathology are also found in DMD muscle. DMD biopsies reveal the presence of mononuclear cells that surround individual myofibers (McDouall et al. 1990). The predominant cell types found in the muscle biopsies of DMD patients include CD4<sup>+</sup> and CD8<sup>+</sup> T-cells, as well as macrophages, although natural killer (NK) cells and dendritic cells (DCs) are also present (McDouall et al. 1990). FOXP3<sup>+</sup> T-regs are also elevated in DMD patients (Villalta et al. 2014). These findings provide evidence that inflammatory infiltrates also play significant roles in DMD pathophysiology. Accordingly, the standard care for patients with DMD has been anti-inflammatory corticosteroids, including prednisone. Prednisone prolongs ambulation and maintains muscle strength in patients (Yilmaz et al. 2004) by potentially inhibiting muscle proteolysis (Kawai et al. 1993). Treatment also reduces leukocyte populations in *mdx* mice, thus confirming its anti-inflammatory effect (Wehling-Henricks et al. 2004). These effects are potentially due to decreased expression of cellular adhesion molecules necessary for leukocyte extravasation, including selectins and ICAM-1, following prednisone treatment in *mdx* mice (Wehling-Henricks et al. 2004). Prednisone treated *mdx* mice also exhibit reduced sarcolemmal

membrane damage (Wehling-Henricks et al. 2004). Despite this, there are several off-target, non-immunosuppressive effects associated with treatment. For example, prednisone affects myogenesis in patients and also induces atrophic pathways in muscle tissue (Quatrocelli et al. 2017). Patients also experience increased weight gain and declined growth rates (Merlini et al. 2003). Because Prednisone can diminish pro-regenerative immune responses and produce several non-target effects in patients, immunomodulatory therapies that lack these negative side effects could have tremendous therapeutic potential in advancing the treatment of DMD.

The goal of this project was to identify a therapy that could modulate the immune response in dystrophic muscle to reduce *mdx* pathology, considering the knowledge gaps described above. We sought an existing immunomodulatory drug that lacked the off-target effects that impair muscle regeneration. The activity of several immune cells relies upon costimulatory molecules that induce myeloid and lymphoid cell activity. Interactions such as these could serve as critical mediators of DMD pathology. For example, T-cell activation relies upon antigen presentation, from APCs such as macrophages, in which the T-cell receptor (TCR) binds to antigen and is presented on MHC expressed on the surface of the APC following antigen processing (Birmingham et al. 1982) (Fig. 1). This interaction alone is not sufficient to initiate an immune response. Costimulatory interaction between members of the B7 family (e.g., CD80 and CD86) interacting with T-cell surface molecule CD28, is required as a “second signal” to induce an immune response (Lenschow et al. 1996) (Fig. 1). Failure of costimulatory interactions results in T-cell anergy, a state in which T-cells are functionally inactive and unable to respond to antigen (Harding et al. 1992). Aside from CD28, cytotoxic T-lymphocyte-associated protein 4 (CTLA-4) serves as a potent negative regulator of immune system activity (Walunas et al. 1994). CTLA-4

and CD28 are homologous receptors expressed on T cells that play opposing roles on T-cell activation (Walunas et al. 1996). Because the binding affinity of CTLA4 greatly exceeds the binding affinity of CD28 for CD80 and CD86, CTLA-4 blocks CD80/86:CD28 interaction, thereby preventing costimulation (Cross et al. 1995) (Fig. 1).

Based on our understanding of costimulatory interactions between leukocyte populations, and the potential of such interactions regulating DMD pathology, we tested a recombinant fusion protein, CTLA4-Ig, that consists of extracellular CTLA4 bound to the Fc portion of IgG (Nafajian et al. 2000) (Fig. 1). CTLA4-Ig has been approved for the treatment of patients as young as two years of age for juvenile idiopathic arthritis (Ruperto et al. 2008). Since DMD is a disease of the childhood, treatments must begin at an early age. The U.S. FDA approval of CTLA4-Ig for juvenile arthritis is an indication of safety and tolerability of the drug in children. These findings were the motivation for our study. Furthermore, there now exists several reports that indicate that CTLA4-Ig may have direct effects on fibrogenic and pro-fibrotic myeloid cells upon B7 receptor binding (Cutolo et al. 2009, Cutolo et al. 2018) (Fig. 1). Interestingly, these effects may occur independent of T-cell costimulation. Since these cells play a major role in DMD pathology, we investigated the effects of CTLA4-Ig treatments on fibrosis in *in vivo* and *in vitro* models pertaining to DMD. We hypothesized that CTLA4-Ig could reduce fibrosis in *mdx* mice and thus, serve as a potential therapeutic intervention for DMD. The findings of this study could possibly lead to the future use of CTLA-4 targeted therapies in the effective treatment of muscular dystrophy and could provide therapeutic insight for similar conditions and diseases for further applications.

## **Materials and Methods**

### Animals

All animal experimentation complied with guidelines established by the UCLA Animal Research Committee. *Mdx* and C57BL/6J mice were purchased from the Jackson Laboratory and bred and housed in a pathogen-free vivarium. Further details of animal care and maintenance have been described elsewhere (Welc et al. 2019).

*Mdx* mice were treated with either IgG (BioXCell) or CTLA4-Ig (BioXCell) intraperitoneally at a dosage of 10 µg, 25 µg, or 50 µg per gram body weight on days 23, 25, and 27 following birth. The mice were later sacrificed at either 4-weeks or 3-months of age. The hind limb muscles of the right leg were frozen in liquid nitrogen-cooled isopentane for histological analysis. The hind limb muscles of the left leg were frozen in liquid nitrogen for qPCR analysis.

### Immunohistochemistry

Macrophage density as well as collagen types I, III, and V accumulation in 4-week and 3-month *mdx* quadriceps muscles. Cross sections (10-µm thickness) of quadriceps muscles were taken from the mid-belly of muscle tissue frozen in isopentane.

The cross sections were fixed in cold acetone for ten minutes and then allowed to air dry for ten minutes. Sections were immersed in phosphate buffered saline solution (PBS) and then incubated in 0.3% hydrogen peroxide in PBS for ten minutes to quench endogenous peroxidase activity. Sections were again washed in PBS and then immersed in solution consisting of 3% bovine serum albumin (BSA), 0.2% gelatin, and 0.05% Tween-20, (blocking buffer), for 30 minutes.

The sectioned tissues were subsequently washed with PBS and then incubated overnight at 4°C in rat anti-CD68 (Serotec 1:100), rat anti-CD206 (BioRad 1:50), rabbit anti-collagen type I (Chemicon, 1:50), goat anti-collagen type III (Southern Biotech, 1:50), or goat anti-collagen type V (Southern Biotech, 1:50) diluted in blocking buffer solution. Following the primary antibody incubation, the sections were washed in PBS. The sections were incubated in their respective biotinylated antibody diluted in PBS (Vector, 1:200) for 30 minutes, followed by a PBS wash and then incubated in streptavidin-horseradish peroxidase (HRP) diluted in PBS (1:1000) for 30 minutes, followed by a final PBS wash. The sections were then developed with a 3-amino-9-ethylcarbazole (A.E.C.) Peroxidase Substrate Kit (Vector).

Macrophages were quantified in sections by observations through an Olympus BH2 microscope (Center Valley, PA, USA) using a 20x objective lens, with the sections overlaid with a 10 x 10 eyepiece micrometer grid. The number of cells per volume was determined by a stereological technique, determined by counting the number of grid intercepts overlying tissue in the field and multiplying this value by section thickness. The numbers of immunolabeled macrophages were counted and expressed as the number of cells per unit volume in the section.

Collagen accumulation was quantified in sections observed through an Olympus BX50 microscope using a 20x objective lens and an eyepiece micrometer grid. The number of total grid intercepts overlying tissue in the field and the number of intercepts overlying tissue positively stained with collagen types I, III, or V were counted. The number of collagen-positive grid intercepts was divided by the total number of intercepts to calculate percent area of collagen.

### Immunofluorescence

Qualitative and quantitative analysis on CD80<sup>+</sup> and HSP47<sup>+</sup> cells in muscle sections using antibodies to CD80 and the collagen chaperone, heat shock protein 47 (HSP47). Cross sections of quadriceps tissues from 4-week and 3-month treated mdx mice were fixed in cold acetone for 10 minutes and then allowed to air dry for 10 minutes. Sections were then blocked with a blocking buffer solution for 30 minutes at room temperature and subsequently washed with PBS, incubated overnight at 4°C with either a hamster anti-CD80 (Biolegend, 1:50) or recombinant rabbit anti-Hsp47 antibody (Abcam, 1:100) in blocking buffer. Following primary antibody incubation, sections were washed in PBS and incubated with biotinylated anti-hamster (Vector 1:100) for CD80 stained sections or anti-rabbit Dylight 488 (Vector, 1:75) for HSP47 stained sections for 30 minutes followed by three PBS washes. The CD80 sections were subsequently incubated with streptavidin 594 (Vector, 1:500) for 30 minutes and washed with PBS. All sections were mounted with ProLong™ Gold Antifade Mount with DAPI and cover slipped. The immunostained sections were quantified using a 20x objective lens using an Olympus BH2 microscope. For cell quantification, previous stereological technique was used to determine the number of cells per unit volume in the section.

### Fibro-adipogenic progenitor cells (FAP) and fibroblast isolation

FAPs were isolated using a method described previously by Welc et al (2019). Fibroblasts were isolated from three-month old C57BL/6J wild-type mice. Quadriceps and hamstring muscles were dissected and rinsed in PBS and minced into a fine slurry then digested in 3 ml of enzyme buffer (Dulbecco's Modified Eagle Medium [DMEM, Sigma], 1% penicillin/streptomycin [P/S], 2.4 U/ml dispase II (Invitrogen), and 1% collagenase, type II (Gibco) per gram of muscle at 37°C

for 40 minutes with gentle shaking and frequent trituration. Sample volumes were raised to 10 ml with DMEM and passed through a 100 µm cell strainer (Falcon). The digestates were then pelleted at 350 g for 5 minutes. Cells were resuspended in 5 ml of fibroblast isolation medium (DMEM, 1% P/S, and 10% fetal bovine serum [FBS]) and pre-plated in collagen- and gelatin-coated culture dishes. The cells were then incubated at 37°C in 5% CO<sub>2</sub> for one hour to allow fibroblasts to adhere to the plate. After the one-hour incubation, plates were washed with PBS to remove non-adherent cells, and 3 ml of fibroblast growth medium were added (DMEM with 1% P/S, and 20% FBS). The cells were incubated at 37°C in 5% CO<sub>2</sub> and fed three times a week with fresh fibroblast growth medium until confluent. When cells were 100% confluent, they were collected for RNA isolation.

#### L929 Fibroblast Assay

To assess fibrotic gene expression of fibroblasts treated with CTLA4-Ig, murine L929 fibroblasts were grown in Eagle's Minimum Essential Medium (EMEM, ATCC) containing 20% FBS at 37°C in 5% CO<sub>2</sub>. The cells were fed three times per week with fresh fibroblast growth medium until 95% confluent. When cells were 95% confluent, they were treated with either 100 µg/ml IgG (BioXCell) or 100 µg/ml CTLA4-Ig (BioXCell) for three-hour incubation at 37°C in 5% CO<sub>2</sub> followed by harvesting of cells for RNA isolation.

## RNA isolation

RNA was isolated from 50 mg of frozen quadriceps muscles after homogenization in Trizol (Life Technologies). Homogenized samples were centrifuged at 12,000 g for 10 minutes at 4°C to pellet insoluble material. The supernatant containing the RNA was incubated at room temperature for five minutes to allow the dissociation of nucleoprotein complexes. Chloroform at 20% of the original Trizol volume was added to each sample and incubated for three minutes at room temperature. The samples were centrifuged at 12,000 g for 15 minutes at 4°C to fractionate them into three distinct layers: organic, phenol-CHCl<sub>3</sub> phase (red and located at the bottom), protein phase (white and located in the middle), and aqueous RNA phase (clear and located at the top). The top aqueous layer containing the RNA was drawn and transferred into a new tube, where an approximately 50% of the original Trizol volume of isopropyl alcohol was added. The samples were mixed by inversion and then incubated at room temperature for 10 minutes. The samples were then centrifuged at 12,000 g for 15 minutes at 4°C, to yield an RNA pellet. The pellet was resuspended in 1 ml of 75% ethanol and centrifuged at 12,000 g for 10 minutes at 4°C. After centrifugation, the supernatant was removed, and the pellet was air dried on ice. Dried pellets were resuspended in RNase-free water. RNA samples were purified with RNeasy Mini Kit (Qiagen). RNA concentrations were determined using a Beckman DU730 spectrophotometer (Beckman Coulter) at wavelengths of 260 nm and 280 nm. All samples had a 260/280 ratio greater than 2.0; RNA quality was assessed via 1.2% agarose gel electrophoresis.

To isolate RNA from FAPs and fibroblasts, growth medium was removed, and cells were washed with cold DPBS. Cells were then replaced with 1 ml of Trizol per sample and were detached with a cell scraper and lysed using a 23-gauge syringe. All subsequent steps for RNA

isolation starting from centrifugation to pelleting insoluble material and resuspension of RNA pellets with RNase-free water were similar to those described above. RNA from FAPs and fibroblasts isolated from quadriceps muscles were purified with RNeasy Mini Kit (Qiagen) according to manufacturer's instructions. RNA concentrations were determined using a Beckman DU730 spectrophotometer (Beckman Coulter) at wavelengths of 260 nm and 280 nm. All samples had a 260/280 ratio greater than 2.0, and RNA quality was assessed via 1.2% agarose gel electrophoresis.

#### Quantitative real-time polymerase chain reaction (qPCR)

Briefly, to generate cDNA, a master-mix consisting of Oligo(dT)<sub>12-18</sub> primer (Invitrogen) and 10 mM dNTPs was added to the samples containing either 1 or 2 µg of RNA and then incubated at 65°C for five minutes. Then a reverse transcriptase master-mix consisting of SuperScript™ II RT (Invitrogen), First-Strand Buffer (Invitrogen), 0.1 M dithiothreitol (Invitrogen), and nuclease-free H<sub>2</sub>O was added to each sample. The samples were then incubated at 42°C for 50 minutes then at 70°C for 50 minutes to heat inactivate the enzyme. The final cDNA sample was diluted 1:1 in sterile water and stored at -20°C.

qPCR analysis was performed using 96-well plates with each well containing 2 µl of cDNA and 23 µl of a master mix (autoclaved water, SYBR® Green Supermix (Bio-Rad) and the corresponding forward and reverse primers for the genes of interest (Table 1). Reference genes used were Srp14 and Rpl13a for all tissue and cell samples. Experiments were performed on a Quantstudio 5 Real-Time PCR System (Thermo Fisher).

## Statistical analysis

All statistical analyses were performed using unpaired Student t-tests or one-way ANOVA with differences considered significant at  $p < 0.05$ . All graphs display mean  $\pm$  standard error of the mean (SEM).

<b>Gene</b>	<b>5' to 3' Sequence</b>
<b>Arginase 1 F</b>	CAATGAAGAGCTGGCTGGTGT
<b>Arginase 1 R</b>	GTGTGAGCATCCACCCAAATG
<b>Arginase 2 F</b>	GAAGTGGTTAGTAGAGCTGTGTC
<b>Arginase 2 R</b>	GGTGAGAGGTGTATTAATGTCCG
<b>TGFb1 F</b>	CTCCACCTGCAAGACCAT
<b>TGFb1 R</b>	CTTAGTTTGGACAGGATCTGG
<b>CD80 F</b>	CTCTTTGTGCTGCTGATTCGTC
<b>CD80 R</b>	GTTTCCCAGCAATGACAGACAG
<b>CD86 F</b>	CTCTTTCATTCCCGGATGGTG
<b>CD86 R</b>	GAGGGCCACAGTAACTGAAGCTG
<b>Col1a1 F</b>	TGTGTGCGATGACGTGCAAT
<b>Col1a1 R</b>	GGGTCCCTCGACTCCTACA
<b>Col3a1 F</b>	ATCCCATTTGGAGAATGTTGTGC
<b>Col3a1 R</b>	GGACATGATTCACAGATTCCAGG
<b>Col5a3 F</b>	CGGGGTACTCCTGGTCCTAC
<b>Col5a3 R</b>	GCATCCCTACTTCCCCCTTG
<b>CTGF F</b>	GGACACCTAAAATCGCCAAGC
<b>CTGF R</b>	GGCACAGGTCTTGATGAACATC
<b>FN F</b>	GCTCAGCAAATCGTGCAGC
<b>FN R</b>	CTAGGTAGGTCCGTTCCCCTG
<b>PDGFRa F</b>	CACGTTTGAGCTGTCAAC
<b>PDGFRa R</b>	CTGGCCAAAACGTGCCACG
<b>Rnps1 (HKG) F</b>	AGGCTCACCAGGAATGTGAC
<b>Rnps1 (HKG) R</b>	CTTGGCCATCAATTTGTCCT
<b>Srp14 (HKG) F</b>	AGAGCGAGCAGTTCCTGAC
<b>Srp14 (HKG) R</b>	CGGTGCTGATCTTCCTTTTC
<b>Rpl13a (HKG) F</b>	CCTGCTGCTCTCAAGGTTGTT
<b>Rpl13a (HKG) R</b>	CGATAGTGCATCTTGGCCTTT
<b>Tpt1 (HKG) F</b>	GGAGGGCAAGATGGTCAGTAG
<b>Tpt1 (HKG) R</b>	CGGTGACTACTGTGCTTTTCG

Table 1. Primer sequences

## Results

### Dose-dependent effects of CTLA4-Ig on muscle inflammation.

We first examined the effects of a range of CTLA4-Ig doses on inflammation in *mdx* muscle, based on dosing used previously in other pre-clinical models of chronic inflammation. Treatment effects were determined by assaying effects on expression of cytokines that play important roles in promoting damage (IFN $\gamma$ ) or repair (IL10) of *mdx* muscle (Villalta et al. 2011). Our results showed that the low dose (10  $\mu$ g/g) produced no significant differences in IFN $\gamma$  and IL-10 expression in quadriceps muscles of CTLA-4 treated mice compared to control IgG-treated mice. At the intermediate dosage (25  $\mu$ g/g) CTLA4-Ig produced a significant 25% reduction in IFN $\gamma$  expression, and a strong trend for a 50% increase in IL-10 expression. At the highest dosage (50  $\mu$ g/g), significant reductions in the expression of IFN $\gamma$  (40%) and IL10 (50%) occurred in CTLA4-Ig treated mice.

Because CTLA4-Ig treatment may also directly affect the activity of macrophages (Cutolo et al. 2009), we examined the effect of CTLA4-Ig *in vivo* on macrophage cell numbers in *mdx* skeletal muscle. At each dose, CTLA4-Ig treated mice had significantly fewer pro-inflammatory CD68<sup>+</sup> macrophages ( $p < 0.05$ ) (Fig. 2A-C). We also examined the number of anti-inflammatory, CD206<sup>+</sup> M2 macrophages in quadriceps of *mdx* mice treated with CTLA4-Ig. Muscles of mice treated with 10  $\mu$ g/g CTLA4-Ig contained significantly more CD206<sup>+</sup> macrophages than IgG treated mice ( $p < 0.05$ ). However, there was no significant effect on numbers of CD206<sup>+</sup> macrophages between CTLA4-Ig and IgG treated *mdx* mice at doses of 25 and 50  $\mu$ g/g ( $p > 0.05$ ) (Fig. 3A-C). Based on these findings, we performed subsequent experiments using 25  $\mu$ g/g, because that concentration reduced IFN $\gamma$  expression, tended to increase IL10 expression, and reduced numbers of CD68<sup>+</sup> macrophages without reducing CD206<sup>+</sup> macrophage numbers.

*CTLA4-Ig treatments reduce pro-fibrotic macrophages and reduce muscle fibrosis.*

Fibrosis is a pathological hallmark of DMD. We thus performed quantitative immunohistochemistry to examine whether CTLA4-Ig had any effect on macrophages associated with fibrosis in dystrophic muscle. CD163, a macrophage activation marker associated with fibrogenesis, was used to identify pro-fibrotic M2 macrophages in *mdx* muscle (Kazankov et al. 2014). Our findings showed that CTLA4-Ig significantly reduced the number of CD163<sup>+</sup> macrophages in 4-weeks of treatment compared to controls ( $p < 0.05$ ) (Fig. 4A and C). A downward trend in CD163<sup>+</sup> density was also found even after 3-months of CTLA4-Ig treatment in *mdx* mice, although this reduction in CD163<sup>+</sup> numbers was not statistically different from IgG treated mice at 25  $\mu\text{g/g}$  ( $p = 0.14$ ) (Fig. 4B). Because macrophages promote fibrosis in *mdx* dystrophy (Wehling-Henricks et al. 2010), these reductions in numbers of CD163<sup>+</sup> cells suggest that CTLA-4 could potentially reduce fibrosis in dystrophic muscle.

We then examined the effect of CTLA4-Ig treatments on collagen accumulation in *mdx* skeletal muscle. In the 4-weeks treatment group, no difference was observed in the percent area of collagens I, III, or V, between IgG and CTLA4-Ig treated *mdx* mice ( $p > 0.05$ ) (Fig 5A-F). However, following 3-months of treatment, a significant reduction in collagens I and V accumulation was found in CTLA4-Ig treated mice ( $p < 0.05$ ) (Fig 6A-F).

Reductions in collagen accumulation in muscles of CTLA4-Ig treated mice are not reflected by reductions in collagen expression in muscle.

We then examined the expression of fibrogenic genes in CTLA4-Ig treated *mdx* mouse muscle. We measured relative gene expression of fibrotic genes in quadriceps whole muscle by qPCR analysis. No statistically significant differences were found in the expression of collagen genes I or III in muscles of 4-week *mdx* mice treated with CTLA4-Ig (Fig. 11A, B), but a downward trend in collagen V expression was observed ( $p=0.08$ ) (Fig. 11C). In 3-month old *mdx* mice, we similarly found a significant reduction in collagen V expression in CTLA4-Ig treated mice (Fig. 12C), although the expression of collagen genes I and III was not significant between treated and control mice (Fig. 12A,B)

CTLA4-Ig treatments do not affect arginase or TGF $\beta$  expression in dystrophic muscles.

Arginase in macrophages drives fibrosis in *mdx* muscles via the production of pro-fibrotic molecules (Wehling-Henricks et al. 2010). Additionally, TGF $\beta$ , which is also expressed by macrophages, is a well-characterized pro-fibrotic cytokine in dystrophic muscle (Song et al. 2019). We used qPCR analysis to assay relative expression of the arginases and TGF- $\beta$  in *mdx* muscles to assay whether CTLA4-Ig treatments reduced the expression of any of those profibrotic enzymes. We did not find significant differences in arginase 1 or 2 expression in CTLA4-Ig treated mice at either 4-weeks and 3 months compared to IgG controls (Fig. 7 A,B,D,E). However, we did identify a trend for a 25% reduction of TGF- $\beta$  expression in 4-week, CTLA4-Ig treated mice ( $p = 0.15$ ) (Fig. 7 C,F). Overall, the results indicate that the CTLA4-Ig effects on fibrosis are not attributable to inhibition of arginase or TGF $\beta$  expression by macrophages.

*Fibroblasts and FAPs express CD80 at levels comparable to expression levels by macrophages in vitro.*

We extended our analysis to other fibrogenic cell populations that may possibly express costimulatory molecules bound by CTLA-4. Because fibroblasts and FAPs are the primary sources of connective tissue in muscle, we assessed their expression levels of CD80 and CD86 relative to macrophages. We first assayed for expression levels of CD80/86 using bone marrow-derived macrophages (BMDMs) as a positive control for expression. Our results show that cultured fibroblasts express levels of CD80 that are comparable to BMDMs ( $p > 0.05$ ) (Fig 8A). However, CD86 expression on fibroblasts was only 0.2% the level that occurred in BMDMs ( $p < 0.05$ ) (Fig. 8B). We also compared relative levels of CD80/86 between cultured fibroblasts and FAPs. We found no significant difference in CD80 expression, and FAPs expressed even lower levels of CD86 than occurred in cultured fibroblasts (Fig. 8C,D). These results show that both fibroblasts and FAPs express levels of CD80 that are comparable to well-established antigen presenting cells and indicate that they would be capable of binding CTLA4-Ig.

*Fibroblasts within inflammatory lesions in dystrophic muscles express CD80.*

Immunofluorescence analysis confirmed that cells expressing heat shock protein 47 (HSP47), also express the CTLA4-Ig binding ligand, CD80 (Figure 9). HSP47, a procollagen chaperone protein in collagen synthesis, is commonly used marker for collagen producing cells (Ito et al. 2017). Although detection was rare, we found that the majority of HSP47/CD80 co-labeled cells were present in large inflammatory lesions in *mdx* muscle (Figure 9). Nonetheless, these observations indicate that HSP47 expressing fibroblasts, may be targets of CTLA-4 mediated reduction of fibrosis. We thus looked into the mechanisms of these effects by assaying the number of collagen producing HSP47<sup>+</sup> cells in dystrophic skeletal muscle, to further our

observations. We found no significant difference in HSP47<sup>+</sup> cell densities in the quadriceps of CTLA4-Ig treated mice compared to IgG control in both time points of 4-weeks, and 3-months *mdx* mice (Fig. 10A-C).

*CTLA4-Ig treatments of fibroblast in vitro reduces their expression of connective tissue proteins.*

Because fibroblasts in dystrophic muscle express CD80 and CTLA4-Ig reduces the expression of some connective tissue proteins in dystrophic muscle, we assayed whether direct treatment of fibroblast *in vitro* with CTLA4-Ig affected their expression of connective tissue genes. We compared relative fibrotic gene expression of L929 fibroblasts stimulated with Th1 cytokines after three-hour incubation with either 100 µg/ml IgG control or CTLA4-Ig. We found that CTLA4-Ig treated fibroblasts expressed significantly lower levels of collagen type III and fibronectin ( $p < 0.05$ ) (Fig. 13B,F), however we found no significant trends in relative expression of collagens I or V (Fig. 13A,C). These findings suggest that the reduction in fibrosis of muscles of CTLA4-Ig treated *mdx* mice, may be in part mediated through CTLA4-Ig binding by fibroblasts.

## Discussion

The significance of this study lies in the discovery of a potential therapeutic approach to manage pathology in dystrophic muscle by disrupting fibrotic mechanisms. Several therapeutic approaches have been tested in the past; however, none of them have been effective in directly modulating the activity of both immune and fibrogenic cells in dystrophic muscle. The CTLA4-Ig fusion protein was selected as our molecule of interest since it has been proven to be safe in the treatment of juvenile joint disorders, and also due to its ability to regulate the immune response upon direct binding to leukocytes (Cutolo et al. 2009, Ko et al. 2010, Ruperto et al. 2010). Although the exact mechanisms by which CTLA4-Ig reduces pathology in *mdx* muscles are still unknown, the results of this study provide further insights into the role of immune and fibrotic cells in dystrophic muscle.

A primary finding in our investigation is that CTLA4-Ig disrupts the accumulation of macrophages in dystrophic muscle. Although we have not identified the mechanisms leading to this result, previous investigations provide potential mechanistic insights. For example, CTLA4-Ig treatment greatly reduces the expression of chemokines associated with macrophage infiltration such as chemokine ligand 2 (CCL2) in rat models of collagen induced arthritis, and cultured human monocytes (Kliwinski et al. 2005, Bozec et al. 2018). The CCL2-CCR2 axis plays a significant role in the recruitment of monocytic populations to sites of muscle injury, and the genetic ablation of CCL2 receptor leads to considerable defects in muscle regeneration following acute injury (Warren et al. 2004). Additionally, the genetic ablation of CCL2 receptor reduces macrophage infiltration in *mdx* muscle (Mojumdar et al. 2014). Thus, decreased CCL2 expression following CTLA4-Ig treatment may cause reductions in macrophage accumulation in

our model. Additionally, reports have also shown that CTLA4-Ig treatment leads to three-fold increases in apoptotic macrophages *in vitro* (Tono et al. 2017). Thus, further studies in our laboratory will explore the exact mechanisms involved in the reduction of macrophages following CTLA4-Ig treatment.

Our findings not only show that CTLA4-Ig treatment affects macrophage numbers, but treatment may also directly influence the prevalence of distinct macrophage populations. This effect on macrophage subpopulations could have major impacts on *mdx* pathology. For example, at acute stages of pathology, inflammatory infiltrates are comprised mostly of CD68<sup>+</sup> M1 macrophages that promote muscle cell lysis, whereas at later regenerative stages, the macrophage populations shift predominantly to CD206<sup>+</sup> M2 macrophages that promote tissue regeneration (Villalta et al. 2011). Because CD68<sup>+</sup> M1 macrophages promote tissue damage, the observed reduction in accumulation could potentially ameliorate dystrophic pathology. In contrast, our results show that CD206<sup>+</sup> M2 macrophages increased significantly at low doses (10 µg/g) of CTLA4-Ig treatment, but there was no treatment effect at higher doses (25 µg/g and 50 µg/g). These results are consistent with reports that CTLA4-Ig treatment can polarize macrophages towards the M2 phenotype in adipose tissue and atherosclerotic lesions (Egen et al. 2002, Fujii et al. 2013, Leitinger et al. 2013). However, although Fujii et al. suggest that CTLA4-Ig treatment induces CD163 expression, we found that CTLA4-Ig treatment reduced CD163<sup>+</sup> numbers in dystrophic muscle. The varying treatment effects on M2 macrophage subpopulations may be due to differences in the activation of CD163<sup>+</sup> and CD206<sup>+</sup> M2 macrophages. CD163<sup>+</sup> expression is increased in response to IL-10 stimulation, whereas CD206<sup>+</sup> expression is upregulated by IL-4 and IL-13 (Mosser et al. 2008). Nonetheless, the reduction in CD163<sup>+</sup> macrophages is important in the

context of dystrophic muscle since this subpopulation of M2 macrophages is associated with tissue fibrosis (Villalta et al. 2009). Altogether, our findings suggest that CTLA4-Ig treatment may support muscle regeneration through the expansion of CD206<sup>+</sup> macrophage populations, while concurrently reducing muscle fibrosis due to the reduction in CD163<sup>+</sup> macrophages.

Our findings that CTLA4-Ig treatment reduced the accumulation of fibrillar collagens are significant, since fibrosis plays a major role in the lethality of DMD (Klinger et al. 2012). In our study, we found reductions in collagens I and V in 3-month old *mdx* mice. Previous studies showed that CTLA4-Ig treatments reduced collagen content and induced regression of pre-existing fibrosis in mouse models of dermal fibrosis (Ponsoye et al. 2016). These findings may be consistent with the observations in our model, since treatment reduced collagens I and V between 4-week and 3-month old mice, while there was no significant difference in collagens between these ages in IgG treated mice (data not shown). Additionally, in 3-month old *mdx* mice, a significant reduction in collagen V expression by qPCR analysis was observed in CTLA4-Ig treated mice. This result was consistent with our collagen % area analysis that showed a reduction in collagen V accumulation. However, reductions in collagen I accumulation were not consistent with our qPCR results following treatment. Since there was no effect on collagen I expression, the result could be due to the observed decreases in collagen V following treatment. Interactions between collagen V and collagen I are critical to regulating fibrillogenesis (Birk et al. 1990). Thus, the reduction in collagen V could potentially lead to diminished structural integrity of type I collagens, and this provides a possible explanation for our observed results on collagen I accumulation. In summary, our findings indicate that CTLA4-Ig treatment can potentially ameliorate pathology by reducing muscle fibrosis in dystrophic muscle.

The observed effects on fibrosis could once again be due to CTLA4-Ig mediated inactivation of monocytic populations in dystrophic muscle. Macrophages contribute to fibrosis by the production of metabolites and cytokines that induce connective tissue accumulation. For example, arginase activity by macrophages promotes muscle fibrosis via these mechanisms in *mdx* muscle (Wehling-Henricks et al. 2010). Additionally, macrophages secrete TGF- $\beta$  during wound healing (Zhu et al. 2017). TGF- $\beta$  is highly correlated with pro-fibrotic processes and is significantly upregulated in DMD muscle (Bernasconi et al. 1997). However, we did not find changes in arginase and TGF- $\beta$  expression following CTLA4-Ig treatment in 4-week and 3-month old *mdx* mice. These results suggest the possibility of other pro-fibrotic and fibrogenic cells potentially affected by CTLA4-Ig binding, in reducing muscle fibrosis in our study.

The activity of non-leukocyte cell populations that contribute to fibrosis may also be influenced by CTLA4-Ig treatment. Although APCs such as macrophages are best characterized for expressing CTLA4 ligands, fibroblasts also express CD80 when stimulated with IFN $\gamma$  and TNF $\alpha$  *in vitro* (Pechold et al. 1997). This suggests that these cells may be a potential target for reducing fibrosis in our model. We thus extended our analysis to fibrogenic cell populations such as fibroblasts and FAPs and confirmed their expression of CTLA-4 binding ligands. Additionally, our *in vivo* observations showed that HSP47/CD80 double-positive cells were present in inflammatory lesions that have robust expression of pro-inflammatory cytokines, including IFN $\gamma$  and TNF $\alpha$  (Villalta et al. 2011). Consistent with these findings, unpublished data from our laboratory has also suggested that FAPs express high levels of costimulatory molecule, CD80. Collectively, these findings highlight that fibrogenic cells could be targets of the CTLA4-Ig

fusion protein and this suggests a possible mechanism for reductions in collagen accumulation, since these cell populations are associated with collagen production (Wahl et al. 1978).

According to their expression of CTLA-4 binding ligands, we sought to determine if the CTLA4-Ig mediated reduction in fibrosis was due to targeted effects on fibroblasts; however, we found no differences in fibroblast numbers between control and treated *mdx* mice. Although no significant reductions were found in HSP47<sup>+</sup> cell densities at either 4-weeks or 3-months of age with treatment, investigations show that CTLA4-Ig treatments reduced myofibroblasts based on alpha-smooth muscle actin ( $\alpha$ SMA) content in murine models of dermal fibrosis (Ponsoye et al. 2016). The differences in findings between the two studies could be attributable to the disease models, dosing, as well as markers for fibroblast/myofibroblast identification. Ponsoye et al. utilized a model for dermal fibrosis induced by bleomycin injections and dosed mice with CTLA4-Ig at 100  $\mu$ g/mice. Additionally, Ponsoye et al. used  $\alpha$ SMA, a well-characterized marker of myofibroblasts (Desmouliere et al. 1993), whereas we used HSP47 as a marker of fibroblasts based on its role as a pro-collagen chaperone protein. Fibrocytes infiltrate inflammatory areas where they differentiate into fibroblasts/myofibroblast via CXCR4/CXCL12 interaction (Liu et al. 2017). A previous study showed that fibrocytes treated with CTLA4-Ig *in vitro* had no effect on CXCR4 expression. Thus, this result is consistent with the HSP47<sup>+</sup> cell densities we observed in CTLA4-Ig treated *mdx* mice.

The therapeutic potential of CTLA4-Ig was further elucidated by comparing our *in vivo* results on fibrotic gene expression to *in vitro* results in which CTLA4-Ig reduced the expression of certain fibrotic genes in L929 fibroblasts *in vitro*. Our study showed reductions in collagen III

and fibronectin expression and trends for reduced expression of collagens I and V. Nevertheless, several inconsistencies were noted between Cutolo et al. and our study. The steady reductions in collagen I expression observed in Cutolo et al. were found in fibrocytes isolated from human systemic sclerosis patients. In our study, CTLA4-Ig treatments were performed on a murine fibroblast cell line. Although fibroblasts are derived from fibrocytes, functional and physiological differences, including discrepancies in the *in vitro* models could explain inconsistencies in results between the two studies. Cutolo et al. observed no changes in expression in collagen I and fibronectin expression in patient fibroblasts stimulated for 24 and 48 hours (Cutolo et al. 2018). Nonetheless, our findings suggest that CTLA4-Ig treatment reduces expression of fibrillar collagen and basement ECM components, suggesting that this may be a mechanism of action of CTLA4-Ig mediated disruption of fibrosis.

Although our study has made several novel findings, the results need to be interpreted in the light of some limitations. Since we found reductions in collagens I and V accumulation, as well as reductions in collagen V expression *in vivo*, we hypothesized that the direct binding of CTLA4-Ig to murine fibroblasts in culture would correlate to those *in vivo* observations. Additionally, large variations that led to non-significant trends in arginase expression prevent us from drawing conclusive evidence that macrophages may also mediate such effects on fibrosis. This translates to the challenge of reproducing results of *in vivo* conditions with *in vitro* cultures. Since we observed trends in collagens I and V expression in CTLA4-Ig stimulated L929 fibroblasts, future studies will be conducted to assess other CTLA-4 concentrations and stimulation periods to enhance the robustness of our findings. *In vitro* experiments will also be performed to investigate the effects of CTLA4-Ig treatments on pro-fibrotic gene expression in stimulated macrophages.

In conclusion, these findings are an essential step toward discovering a new therapeutic approach for DMD. The results of this study provide evidence that the CTLA4-Ig fusion protein may be an effective remedy in reducing excess ECM deposition by inhibiting fibrotic mechanisms, and therefore ameliorates pathology in dystrophic muscle.

**Figure 1**

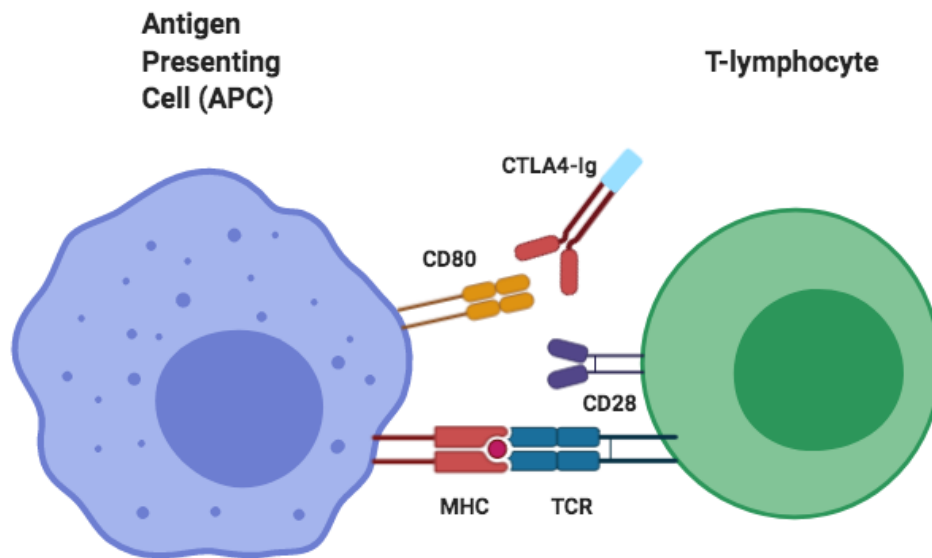


**Figure 1.** CTLA4-Ig disrupts costimulation during naïve T-cell activation. The blockade of CD28-B7 results in increased cell death and anergy of T-cells. The direct binding of CTLA4-Ig to B7 expressed on antigen presenting cells (APCs), including macrophages, may potentially have similar inhibitory effects on these cells, independent of T-cell involvement. These potential effects could play a major modulatory role in the progression of dystrophic pathologies.

**Figure 2**

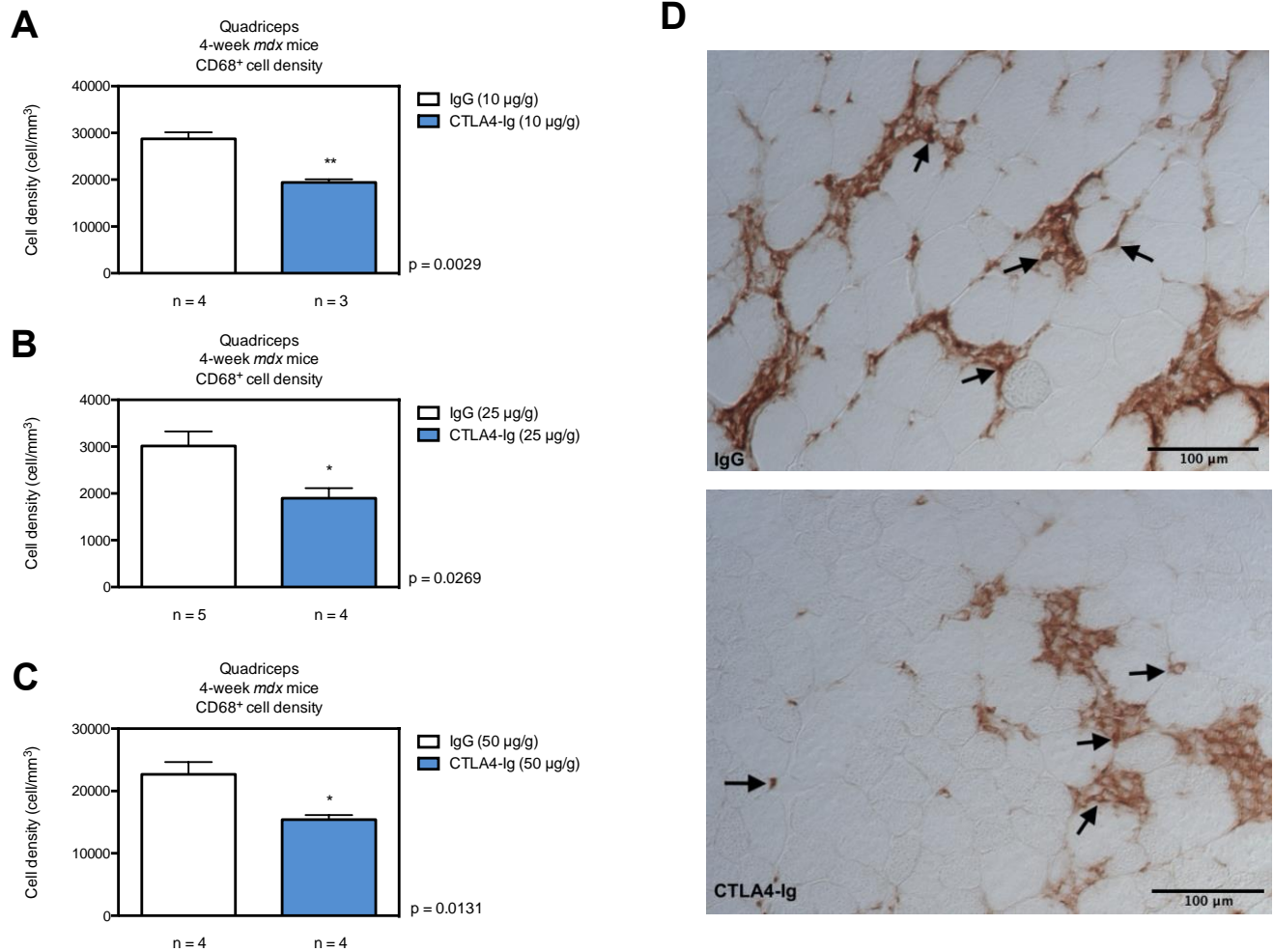


**Figure 2.** CTLA4-Ig treatment reduces pro-inflammatory macrophage numbers in *mdx* mice quadriceps muscle **A-C**) CD68<sup>+</sup> macrophage density in the quadriceps muscles of 4-week *mdx* mice treated with (A) 10 µg/g, (B) 25 µg/g or (C) 50 µg/g CTLA4-Ig compared to IgG treatment at corresponding doses (\* indicates  $p < 0.05$ , \*\* indicates  $p < 0.01$ ) **D**) Representative images of quadriceps muscle of 4-week old 10 µg/g IgG treated mice (top) and 10 µg/g CTLA4-Ig treated mice (bottom); showing vast accumulation of macrophages surrounding necrotic myofibers in IgG treated mice compared to lower density in CTLA4-Ig treated mice. Arrows indicate CD68<sup>+</sup> cells. Data are presented as mean  $\pm$  sem. P values are based on unpaired two-tailed t-test. Scale bar = 100 µm

**Figure 3**

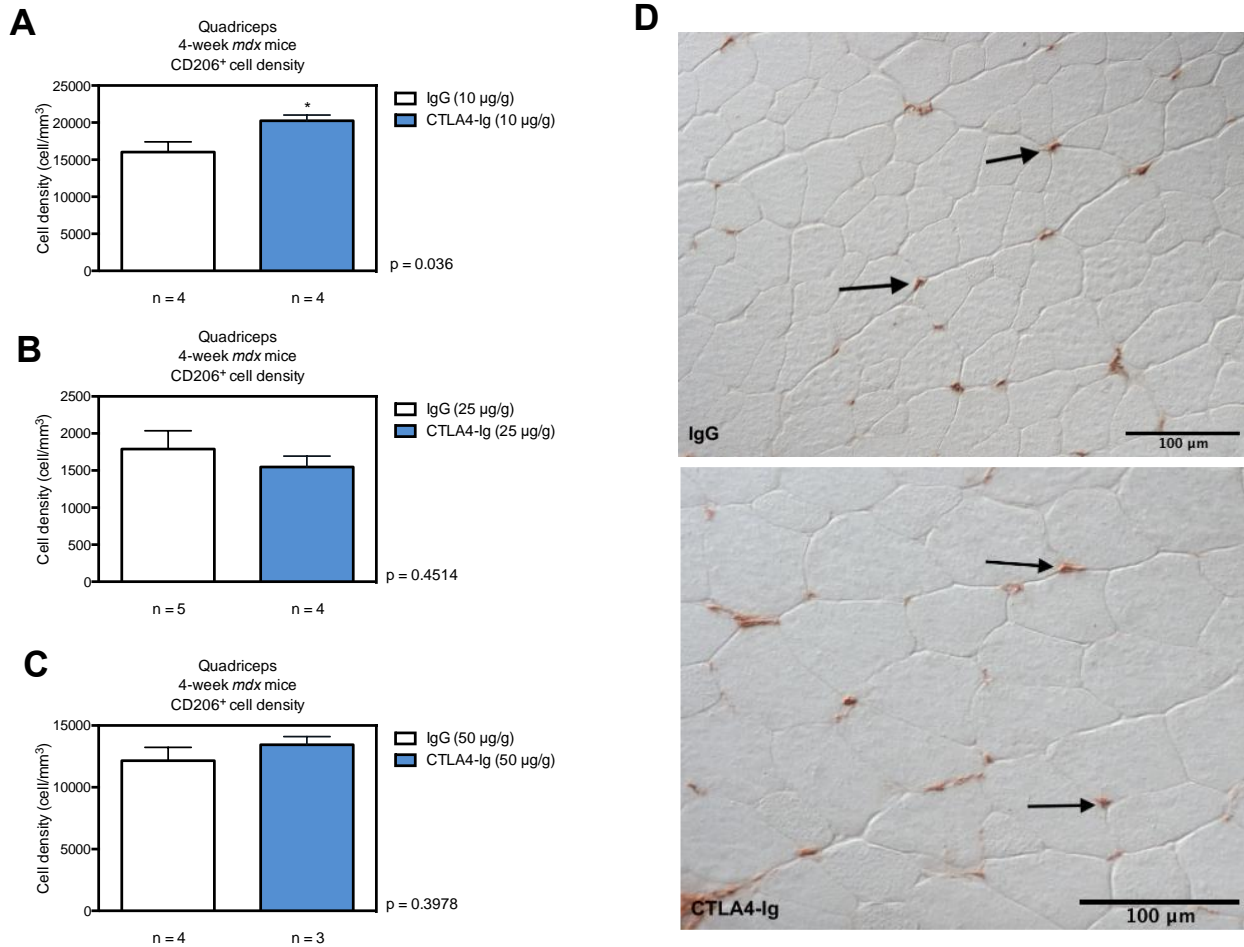


**Figure 3.** CTLA4-Ig treatment does not affect anti-inflammatory macrophage numbers in *mdx* mice quadriceps muscles of intermediate (25 µg/g), and high-dose (50 µg/g) treatment **A-C**) CD206<sup>+</sup> macrophage numbers increased at low-dose CTLA4-Ig treated *mdx* quadriceps compared to low-dose IgG treated *mdx* quadriceps (A). CD206<sup>+</sup> cell density was not affected at the intermediate, and high-dose treatments of 25 µg/g and 50 µg/g, respectively (**B,C**) **D**) Representative images of mice quadriceps muscle at 4-weeks of age, 50 µg/g IgG treated mice (top) and 50 µg/g CTLA4-Ig treated mice (bottom) showing similar distribution of macrophages between control and CTLA4-Ig treated mice. Arrows indicate CD206<sup>+</sup> cells. Data are presented as mean ± sem. P values are based on unpaired two-tailed t-test. Scale bar = 100 µm

**Figure 4**

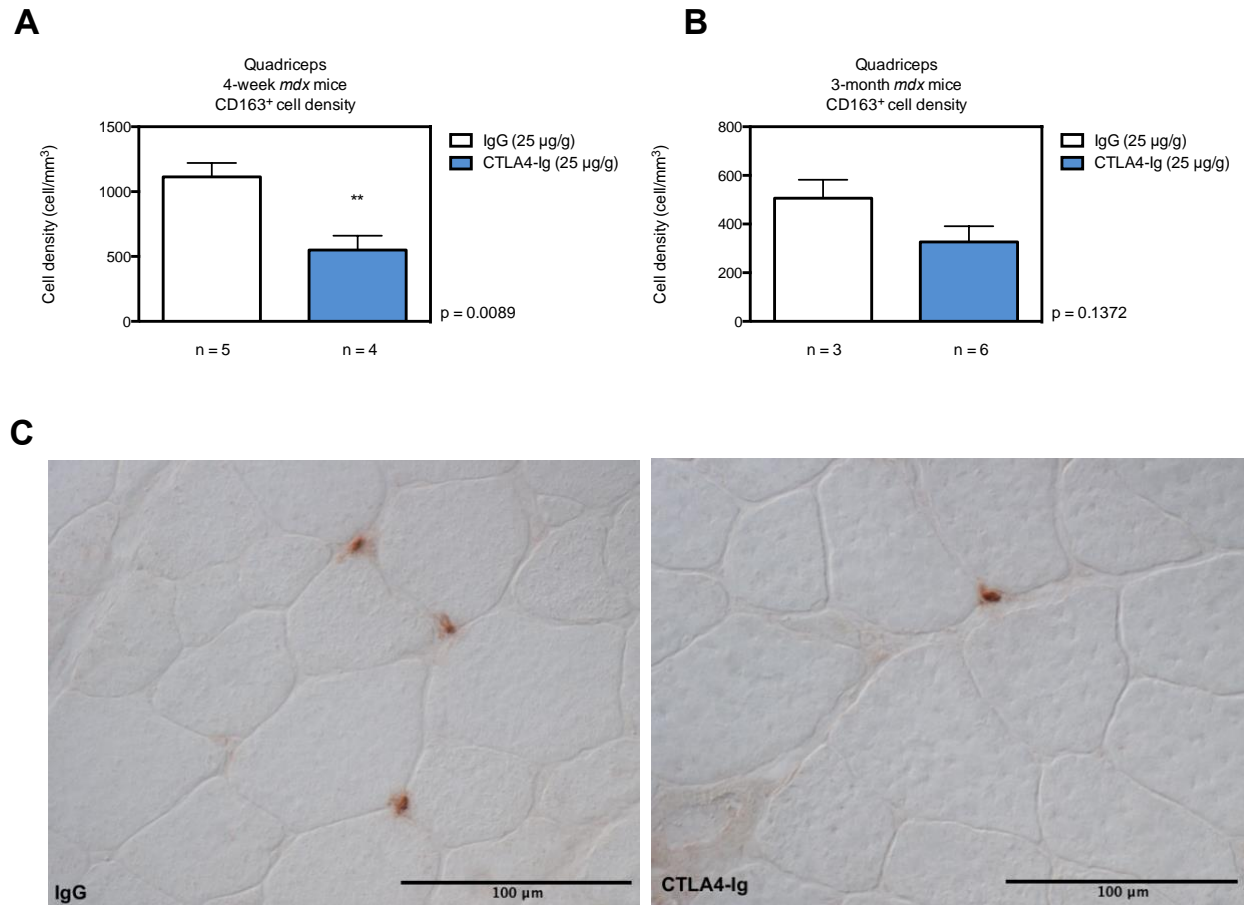


**Figure 4.** CTLA4-Ig treatment reduces pro-fibrotic CD163<sup>+</sup> macrophage numbers in 4-week old *mdx* mice **A-B**) CD163<sup>+</sup> macrophage density reduced in CTLA4-Ig treated *mdx* quadriceps compared to IgG control (A). Additionally, a downward trend in CD163<sup>+</sup> cell density was found in 3-month old *mdx* CTLA4-Ig treated mice compared to control (B) **C**) Representative images of quadriceps muscle of 4-week IgG treated mice (left) and CTLA4-Ig treated mice (right). Data are presented as mean ± sem. P values are based on unpaired two-tailed t-test. Scale bar = 100 µm

**Figure 5**

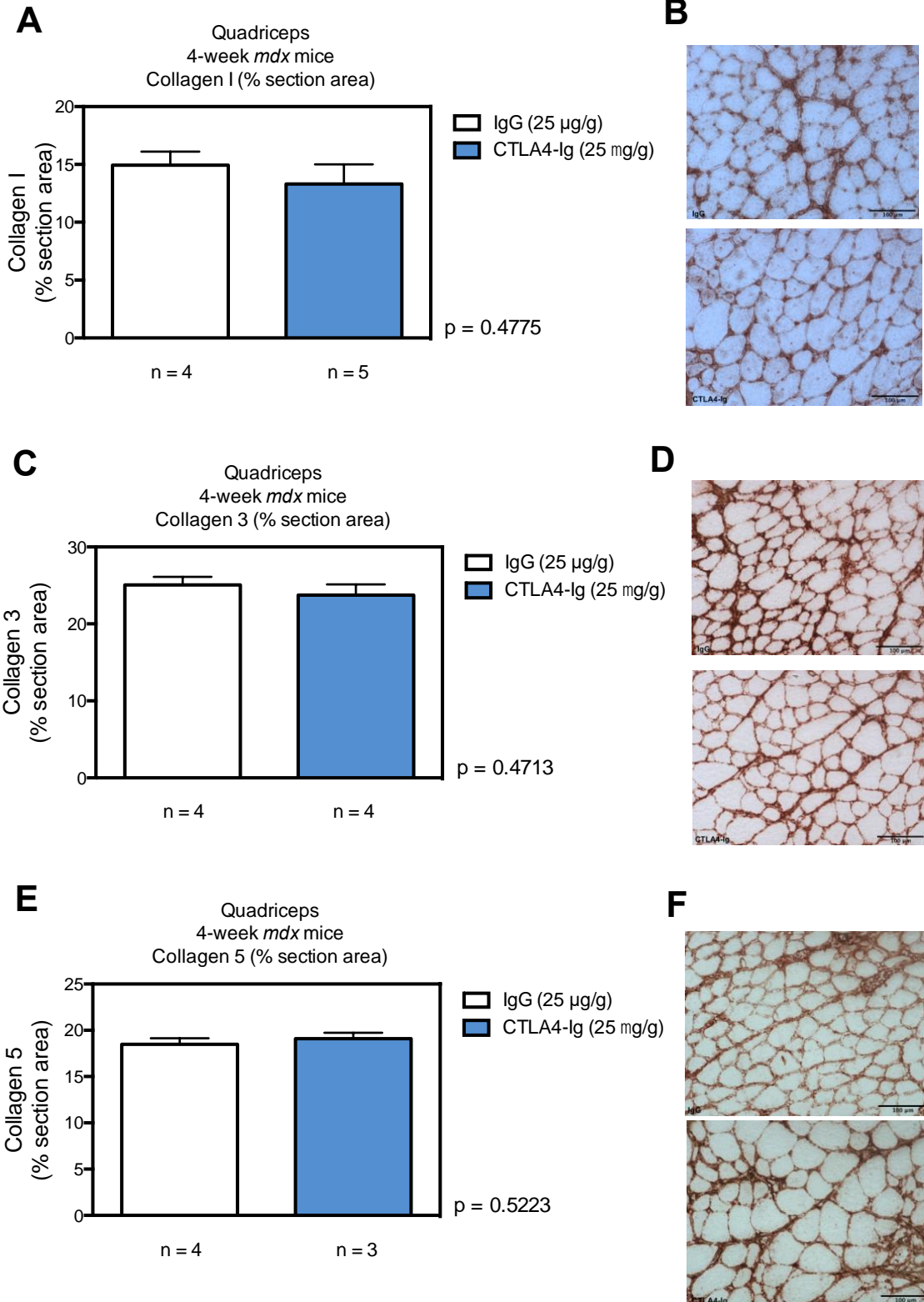


**Figure 5.** CTLA4-Ig does not affect collagen accumulation in 4-week old *mdx* mice. Cross sections of *mdx* mice quadriceps tissue were immunolabeled with anti-collagen type I (**A-B**), anti-collagen type III (**C-D**), and anti-collagen type V (**E-F**). Percent area analysis was conducted in 4-week old *mdx* quadriceps treated with 25  $\mu\text{g/g}$  IgG or CTLA4-Ig for collagen type I (**A**), type III (**C**), and type V (**E**). Representative cross sections of IgG immunolabeled tissue (top) and CTLA4-Ig labeled tissue (bottom) are included for collagen type I (**B**), type III (**D**), and type V (**F**). Data are presented as mean  $\pm$  sem. P values are based on unpaired two-tailed t-test. Scale bar = 100  $\mu\text{m}$

**Figure 6**

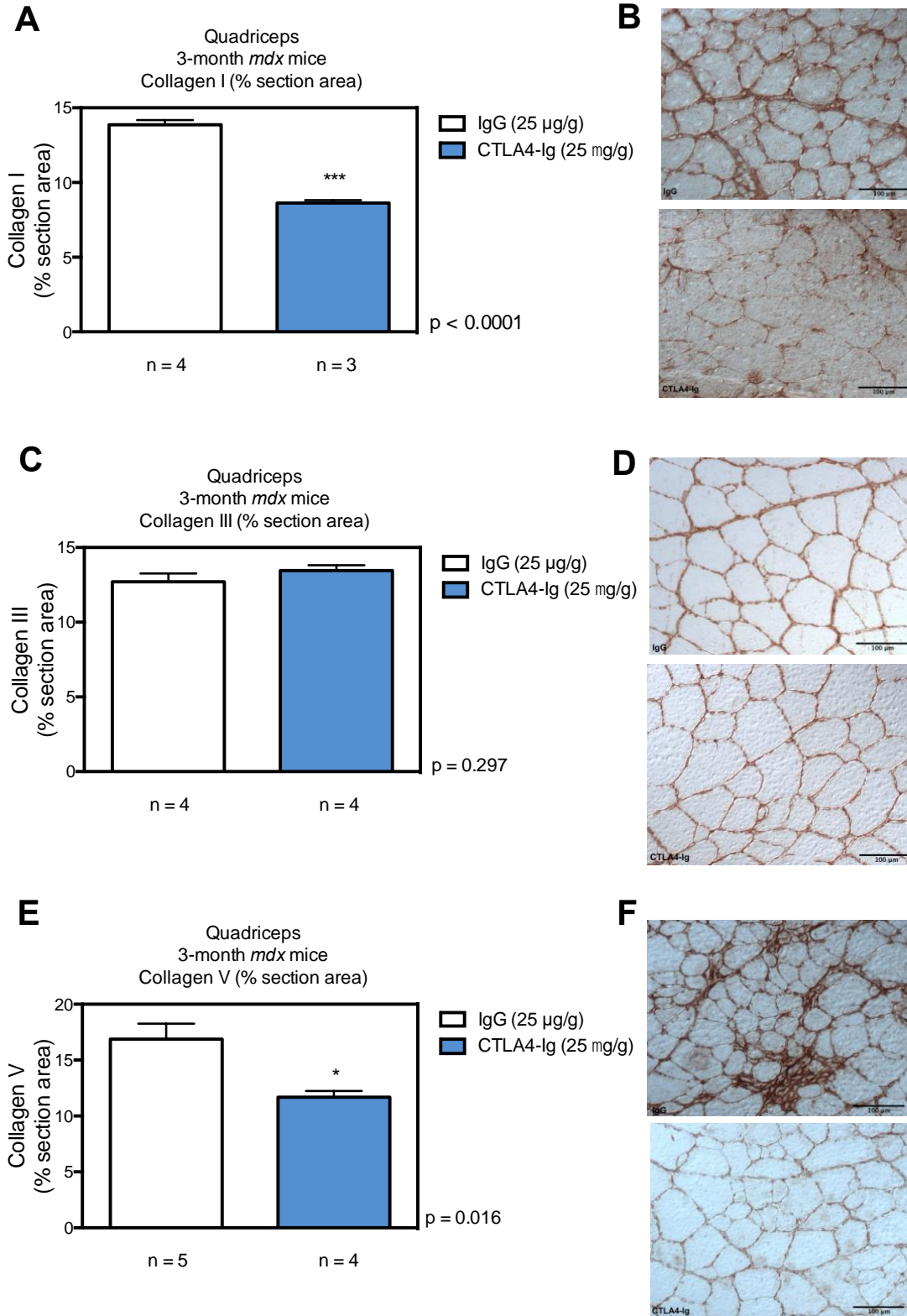


**Figure 6.** CTLA4-Ig treatment reduced collagens I and V accumulation in 3-month old *mdx* mice. Cross sections of *mdx* quadriceps tissue were immunolabeled with anti-collagen type I (**A-B**), anti-collagen type III (**C-D**), and anti-collagen type V (**E-F**). Percent area analysis was conducted in 3-month old *mdx* quadriceps treated with 25  $\mu\text{g/g}$  IgG or CTLA4-Ig for collagen type I (**A**), type III (**C**), and type V (**E**) showed significant reductions in collagens I and V accumulation in CTLA4-Ig treated tissue. Representative cross sections of IgG immunolabeled tissue (top) and CTLA4-Ig labeled tissue (bottom) are included for collagen type I (**B**), type III (**D**), and type V (**F**). (\* indicates  $p < 0.05$ , \*\*\* indicates  $p < 0.001$ .) Data are presented as mean  $\pm$  sem. P values are based on unpaired two-tailed t-test. Scale bar = 100  $\mu\text{m}$

**Figure 7**

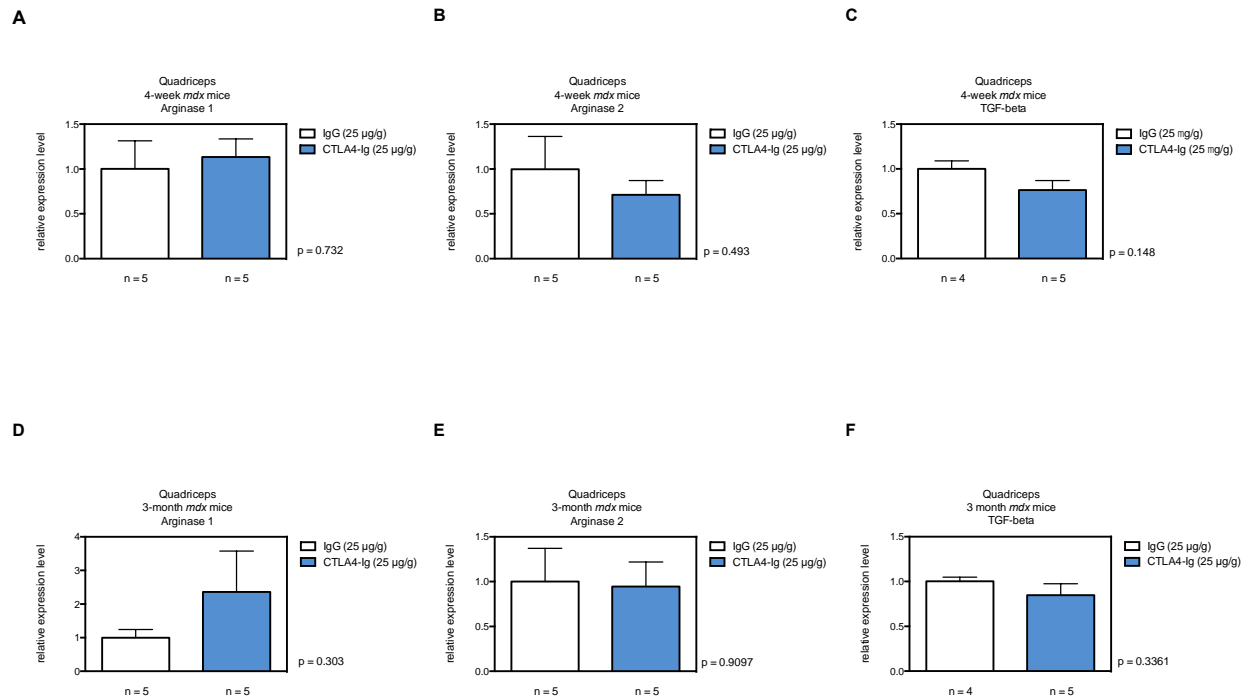


**Figure 7.** Relative mRNA expression of genes associated with fibrosis in macrophages is not affected by CTLA4-Ig treatment in quadriceps of 4-week and 3-month old *mdx* mice **A-F**) qPCR analysis of 4-week (A-C) and 3-month (D-F) old mice *mdx* quadriceps muscles showing no significant difference between IgG and CTLA4-Ig treated mice for relative gene expression including Arginase 1 (**A,D**), Arginase 2 (**B,E**), and TGF- $\beta$  (**C,F**). Data are normalized to IgG control, set at “1” for each gene assayed. Data are presented as mean  $\pm$  sem. P values are based on unpaired two-tailed t-test.

**Figure 8**

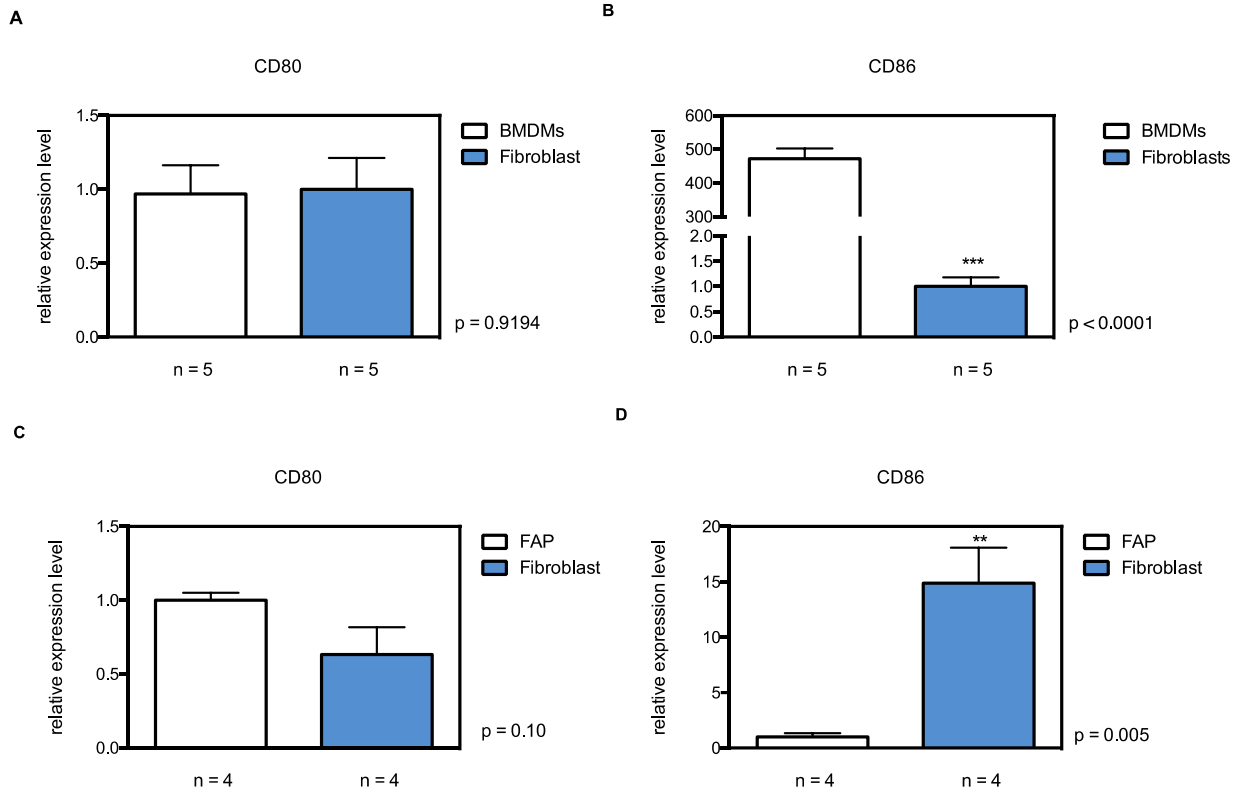


**Figure 8.** Fibrogenic cells express costimulatory molecules **A-B)** Relative CD80/86 mRNA expression levels between bone marrow-derived macrophages (BMDMs) and cultured fibroblasts showing that cultured fibroblasts express comparable levels of CD80 to macrophages, while they do not express CD86. **C-D)** qPCR analysis showing that cultured fibroblasts express high levels of CD86 compared to FAPs (\*\* indicates  $p < 0.01$ , \*\*\* indicates  $p < 0.001$ ). Data are normalized to control, set at “1” for each gene assayed. Data are presented as mean  $\pm$  sem. P values are based on unpaired two-tailed t-test.

**Figure 9**

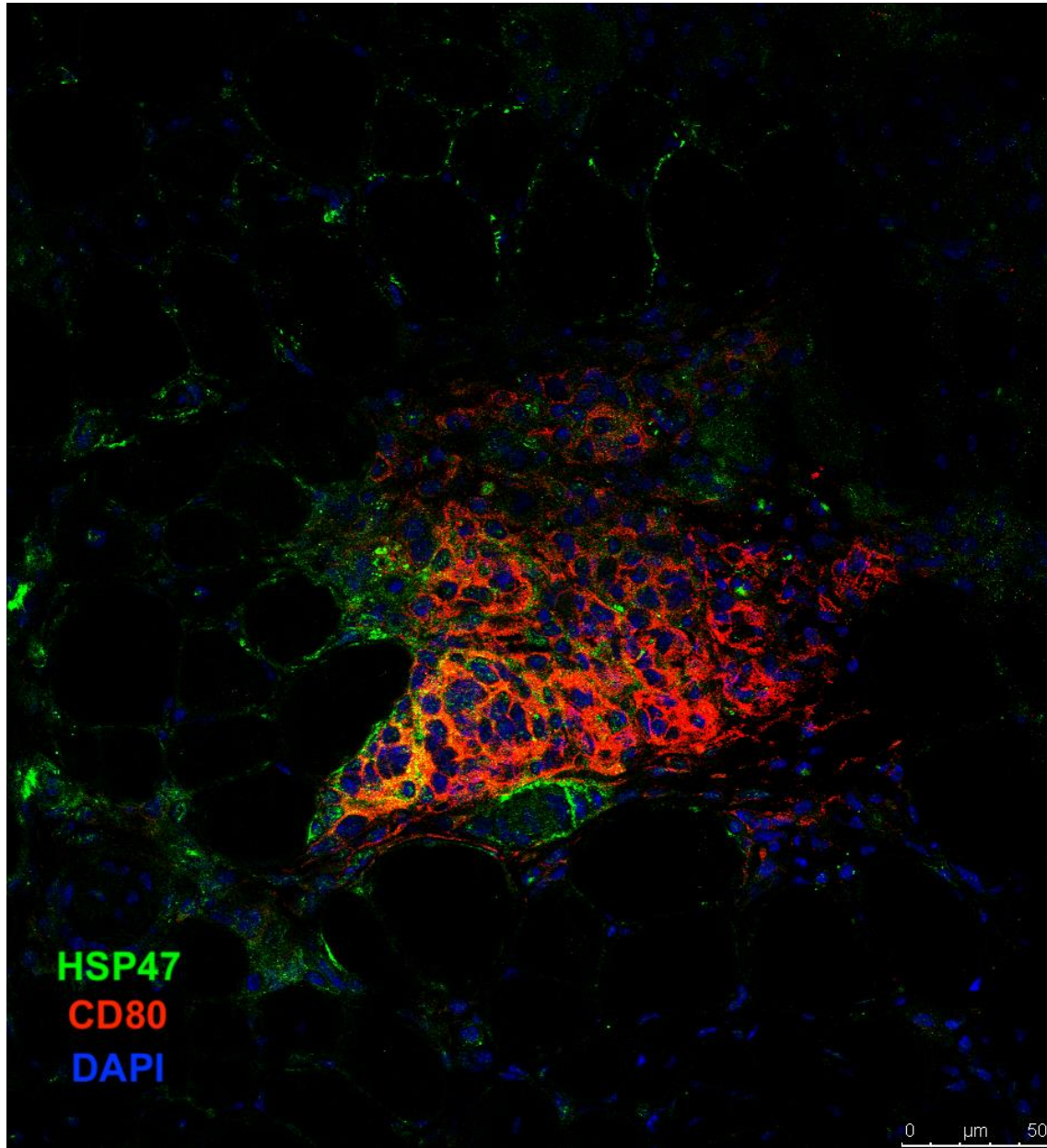


**Figure 9.** HSP47<sup>+</sup> cells express CTLA-4 binding ligand CD80. Confocal image shows that HSP47 expressing cells also express CD80 in *mdx* inflammatory lesions, suggesting that CTLA4-Ig could potentially modulate the activity of HSP47 expressing cells, such as fibroblasts. Scale bar = 50  $\mu\text{m}$

**Figure 10**

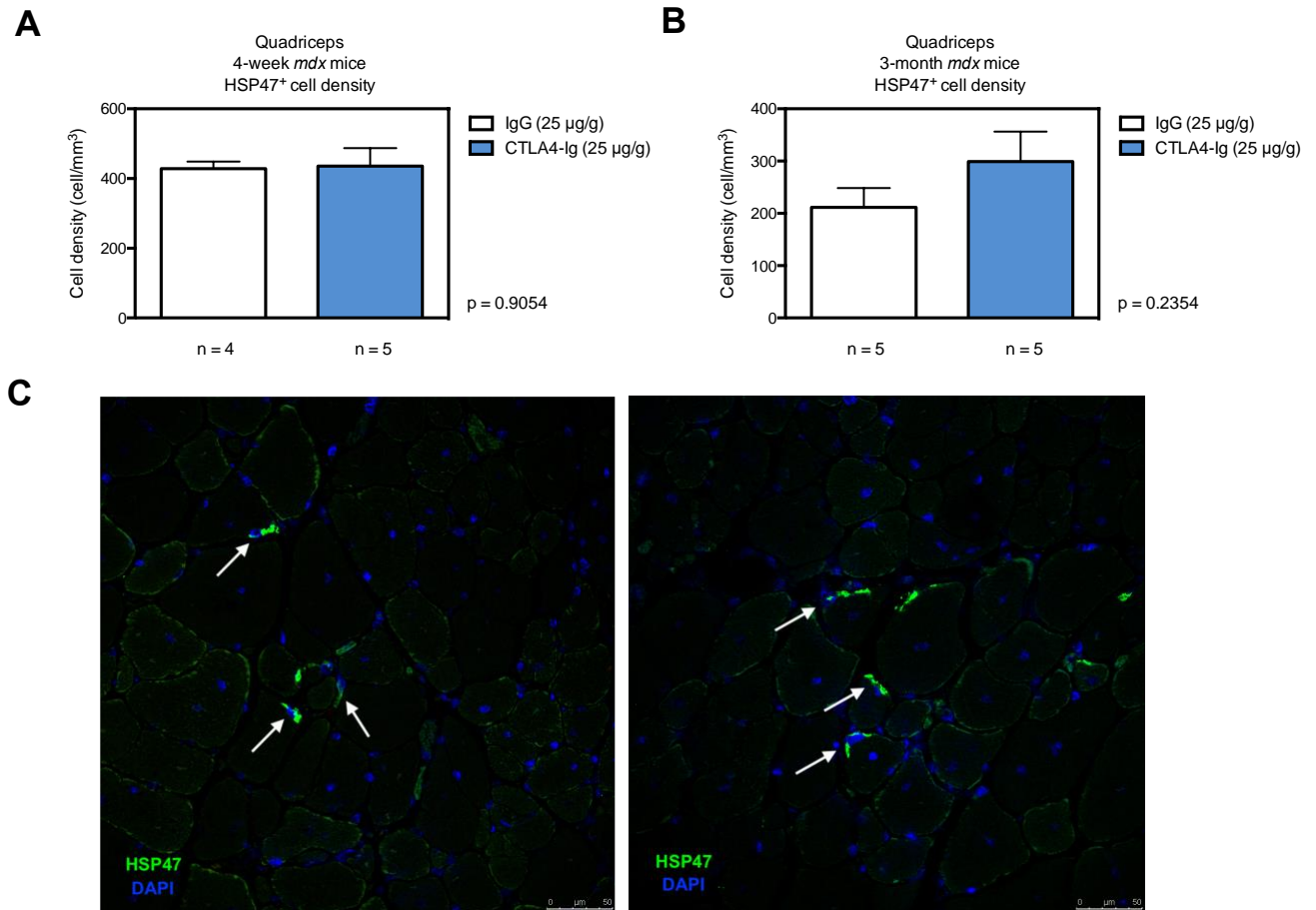


**Figure 10.** CTLA4-Ig treatment has no effect HSP47<sup>+</sup> cell numbers in *mdx* mice. **A-B)** Quadriceps cross sections were immunolabeled with anti-HSP47, and cell densities were analyzed in both 4-week (A) and 3-month (B) old *mdx* mice tissue. Cross sections (C) of anti-HSP47 labeled tissue are included from 4-week old *mdx* mice. Arrows indicate HSP47<sup>+</sup> cells. Data are presented as mean ± sem. P values are based on unpaired two-tailed t-test. Scale bar = 50 µm

**Figure 11**

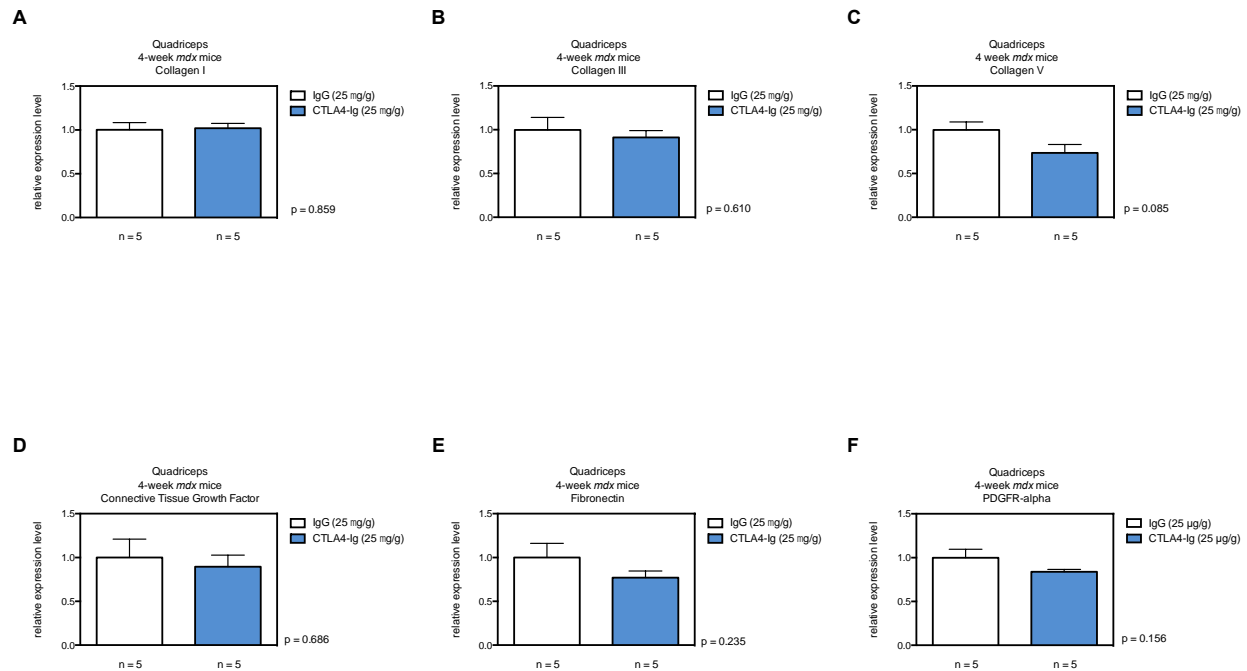


**Figure 11.** Relative mRNA expression of fibrotic genes is not affected by CTLA4-Ig treatment in quadriceps of 4-week old *mdx* mice **A-F**) qPCR analysis of 4-week old *mdx* quadriceps muscles shows no significant difference between IgG treated and CTLA4-Ig treated mice for relative fibrotic gene expression including collagen type I (**A**), type III (**B**), type V (**C**), connective tissue growth factor (**D**), fibronectin (**E**), and PDGFR- $\alpha$  (**F**). Data are normalized to IgG control, set at “1” for each gene assayed. Data are presented as mean  $\pm$  sem. P values are based on unpaired two-tailed t-test.

**Figure 12**

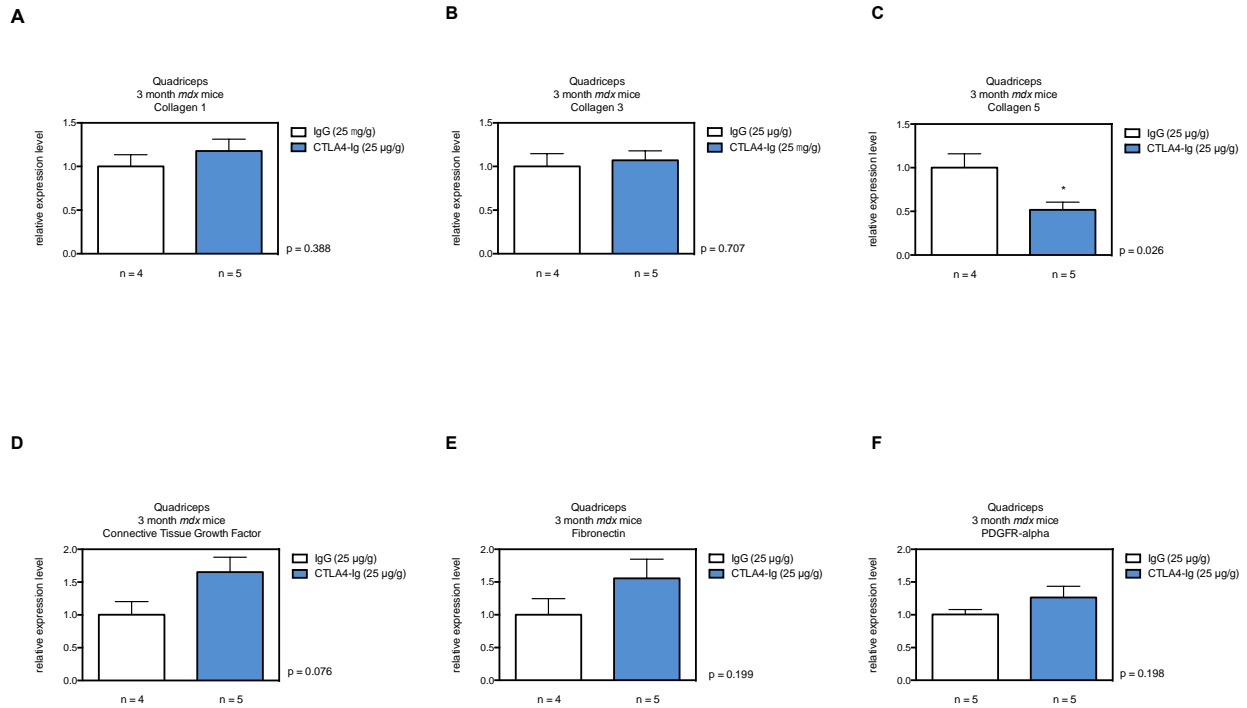


**Figure 12.** Collagen V relative expression is reduced in quadriceps of CTLA4-Ig treated *mdx* mice. qPCR analysis of 3-month old *mdx* mice quadriceps muscles shows a significant reduction in collagen V expression in CTLA4-Ig treated mice compared to IgG treated mice (C). Other genes assayed for relative fibrotic gene expression include collagen type I (A), type III (B), connective tissue growth factor (D), fibronectin (E), and PDGFR- $\alpha$  (F). Data are normalized to IgG control, set at “1” for each gene assayed. (\* indicates  $p < 0.05$ ) Data are presented as mean  $\pm$  sem. P values are based on unpaired two-tailed t-test.

**Figure 13**

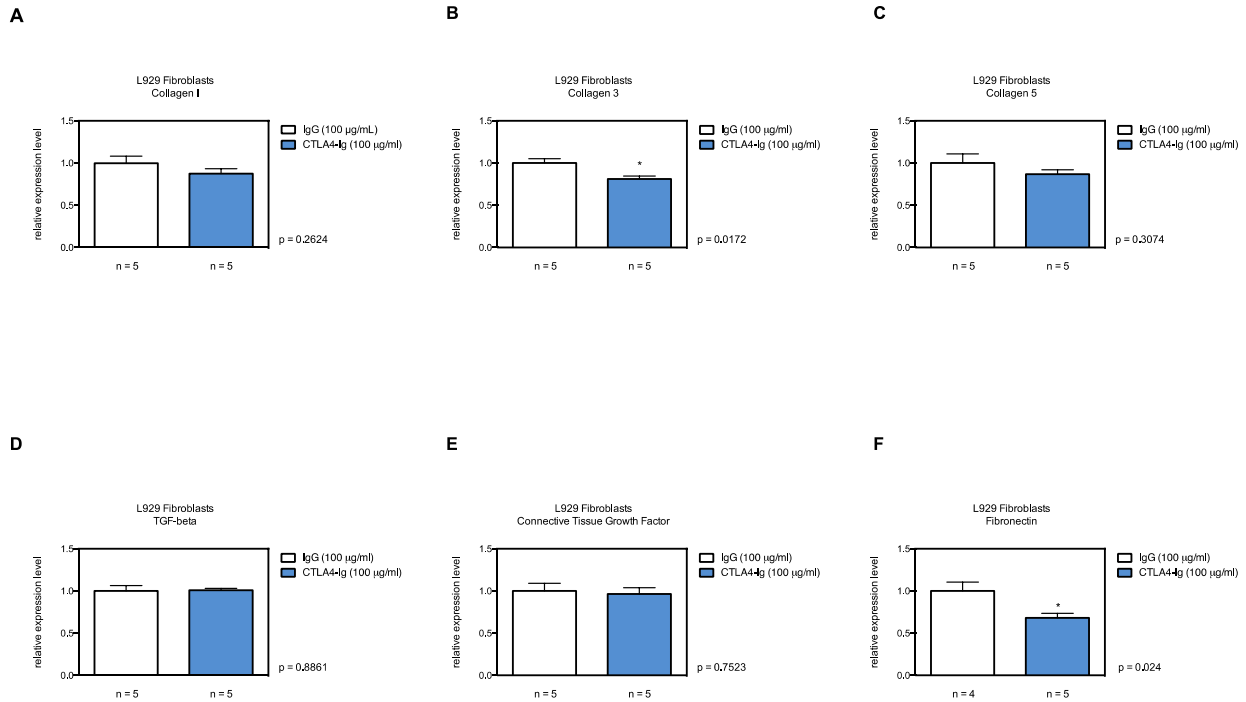


**Figure 13.** Collagen III and fibronectin relative expression is reduced in L929 fibroblasts treated with CTLA4-Ig. qPCR analysis of treated L929 fibroblasts shows a significant reduction in collagen III (B) and FN expression (F) in CTLA4-Ig treated fibroblasts compared to IgG treated fibroblasts. Other fibrotic genes showed trends with CTLA4-Ig treatment for relative fibrotic gene expression include collagen type I (A), collagen type V (C), TGF- $\beta$  (D), and connective tissue growth factor (E). Data are normalized to IgG control, set at “1” for each gene assayed. (\* indicates  $p < 0.05$ ) Data are presented as mean  $\pm$  sem. P values are based on unpaired two-tailed t-test.

## References

1. Andreetta, F., Bernasconi, P., Baggi, F., Ferro, P., Oliva, L., Arnoldi, E., & Confalonieri, P. (2006). Immunomodulation of TGF-beta1 in mdx mouse inhibits connective tissue proliferation in diaphragm but increases inflammatory response: implications for antifibrotic therapy. *Journal of Neuroimmunology*, *175*(1-2), 77-86.
2. Behrens, L., Kerschensteiner, M., Misgeld, T., Goebels, N., Wekerle, H., & Hohlfeld, R. (1998). Human muscle cells express a functional costimulatory molecule distinct from B7. 1 (CD80) and B7. 2 (CD86) in vitro and in inflammatory lesions. *The Journal of Immunology*, *161*(11), 5943-5951.
3. Bernasconi, P., Torchiana, E., Confalonieri, P., Brugnoli, R., Barresi, R., Mora, M., & Mantegazza, R. (1995). Expression of transforming growth factor-beta 1 in dystrophic patient muscles correlates with fibrosis. Pathogenetic role of a fibrogenic cytokine. *The Journal of Clinical Investigation*, *96*(2), 1137-1144.
4. Birk, D. E., Fitch, J. M., Babiarz, J. P., Doane, K. J., & Linsenmayer, T. F. (1990). Collagen fibrillogenesis in vitro: interaction of types I and V collagen regulates fibril diameter. *Journal of Cell Science*, *95*(4), 649-657.
5. Birmingham, J. R., Chesnut, R. W., Kappler, J. W., Marrack, P., Kubo, R., & Grey, H. M. (1982). Antigen presentation to T cell hybridomas by a macrophage cell line: an inducible function. *The Journal of Immunology*, *128*(3), 1491-1492.
6. Bozec, A., Luo, Y., Engdahl, C., Figueiredo, C., Bang, H., & Schett, G. (2018). Abatacept blocks anti-citrullinated protein antibody and rheumatoid factor mediated cytokine production in human macrophages in IDO-dependent manner. *Arthritis Research & Therapy*, *20*(1), 1-9.

7. Brigitte, M., Schilte, C., Plonquet, A., Baba-Amer, Y., Henri, A., Charlier, C., & Chrétien, F. (2010). Muscle resident macrophages control the immune cell reaction in a mouse model of notexin-induced myoinjury. *Arthritis & Rheumatism: Official Journal of the American College of Rheumatology*, 62(1), 268-279.
8. Chen, S. J., Yuan, W., Mori, Y., Levenson, A., Varga, J., & Trojanowska, M. (1999). Stimulation of type I collagen transcription in human skin fibroblasts by TGF- $\beta$ : involvement of Smad 3. *Journal of Investigative Dermatology*, 112(1), 49-57.
9. Chuva De Sousa Lopes, S. M., Feijen, A., Korving, J., Korchynskyi, O., Larsson, J., Karlsson, S., & Mummery, C. L. (2004). Connective tissue growth factor expression and Smad signaling during mouse heart development and myocardial infarction. *Developmental dynamics: An Official Publication of the American Association of Anatomists*, 231(3), 542-550.
10. Contreras, O., Rebolledo, D. L., Oyarzún, J. E., Olguín, H. C., & Brandan, E. (2016). Connective tissue cells expressing fibro/adipogenic progenitor markers increase under chronic damage: relevance in fibroblast-myofibroblast differentiation and skeletal muscle fibrosis. *Cell and Tissue Research*, 364(3), 647-660.
11. Cross, A. H., Girard, T. J., Giacoletto, K. S., Evans, R. J., Keeling, R. M., Lin, R. F., & Karr, R. W. (1995). Long-term inhibition of murine experimental autoimmune encephalomyelitis using CTLA-4-Fc supports a key role for CD28 costimulation. *The Journal of Clinical Investigation*, 95(6), 2783-2789.
12. Cutolo, M., Soldano, S., Montagna, P., Sulli, A., Serio, B., Villaggio, B., & Brizzolara, R. (2009). CTLA4-Ig interacts with cultured synovial macrophages from rheumatoid

- arthritis patients and downregulates cytokine production. *Arthritis Research & Therapy*, 11(6), R176.
13. Cutolo, M., Soldano, S., Montagna, P., Trombetta, A. C., Contini, P., Ruaro, B., & Brizzolara, R. (2018). Effects of CTLA4-Ig treatment on circulating fibrocytes and skin fibroblasts from the same systemic sclerosis patients: an in vitro assay. *Arthritis Research & Therapy*, 20(1), 157.
14. Desguerre, I., Mayer, M., Leturcq, F., Barbet, J. P., Gherardi, R. K., & Christov, C. (2009). Endomysial fibrosis in Duchenne muscular dystrophy: a marker of poor outcome associated with macrophage alternative activation. *Journal of Neuropathology & Experimental Neurology*, 68(7), 762-773.
15. Desmoulière, A., Geinoz, A., Gabbiani, F., & Gabbiani, G. (1993). Transforming growth factor-beta 1 induces alpha-smooth muscle actin expression in granulation tissue myofibroblasts and in quiescent and growing cultured fibroblasts. *The Journal of Cell Biology*, 122(1), 103-111.
16. Ding, L., Linsley, P. S., Huang, L. Y., Germain, R. N., & Shevach, E. M. (1993). IL-10 inhibits macrophage costimulatory activity by selectively inhibiting the up-regulation of B7 expression. *The Journal of Immunology*, 151(3), 1224-1234.
17. Egen, J. G., Kuhns, M. S., & Allison, J. P. (2002). CTLA-4: new insights into its biological function and use in tumor immunotherapy. *Nature Immunology*, 3(7), 611-618.
18. Fielding, R.A., Manfredi, T.J., Ding, W., Fiatarone, M.A., Evans, W.J., Cannon, J.G. (1993) Acute phase response in exercise. III. Neutrophil and IL-1 beta accumulation in skeletal muscle. *The American Journal of Physiology* 265(1 Pt 2): R166-172.

19. Fu, S., Zhang, N., Yopp, A. C., Chen, D., Mao, M., Chen, D., & Bromberg, J. S. (2004). TGF- $\beta$  induces Foxp3<sup>+</sup> T-regulatory cells from CD4<sup>+</sup> CD25<sup>-</sup> precursors. *American Journal of Transplantation*, 4(10), 1614-1627.
20. Fujii, M., Inoguchi, T., Batchuluun, B., Sugiyama, N., Kobayashi, K., Sonoda, N., & Takayanagi, R. (2013). CTLA-4Ig immunotherapy of obesity-induced insulin resistance by manipulation of macrophage polarization in adipose tissues. *Biochemical and Biophysical Research Communications*, 438(1), 103-109.
21. Goldspink, G., Fernandes, K., Williams, P. E., & Wells, D. J. (1994). Age-related changes in collagen gene expression in the muscles of mdx dystrophic and normal mice. *Neuromuscular Disorders*, 4(3), 183-191.
22. Green, A. M., DiFazio, R., & Flynn, J. L. (2013). IFN- $\gamma$  from CD4 T cells is essential for host survival and enhances CD8 T cell function during Mycobacterium tuberculosis infection. *The Journal of Immunology*, 190(1), 270-277.
23. Hahn, K., deBiasio, R., Tishon, A., Lewicki, H., Gairin, J. E., LaRocca, G., & Oldstone, M. (1994). Antigen presentation and cytotoxic T lymphocyte killing studied in individual, living cells. *Virology*, 201(2), 330-340.
24. Harding, F. A., McArthur, J. G., Gross, J. A., Raulet, D. H., & Allison, J. P. (1992). CD28-mediated signalling co-stimulates murine T cells and prevents induction of anergy in T-cell clones. *Nature*, 356(6370), 607-609.
25. Herbst, S., Schaible, U. E., & Schneider, B. E. (2011). Interferon gamma activated macrophages kill mycobacteria by nitric oxide induced apoptosis. *PloS One*, 6(5), e19105.

26. Hoffman, E.P., Brown, R.H.Jr., Kunkel L.M. (1987) Dystrophin: the protein product of the Duchenne muscular dystrophy locus. *Cell*, 51, 919-928.
27. Holness, C. L., & Simmons, D. L. (1993). Molecular Cloning of CD68, a Human Macrophage Marker Related to Lysosomal Glycoproteins. *Blood*, 81(6), 1607-1613.
28. Horsley, V., Jansen, K. M., Mills, S. T., & Pavlath, G. K. (2003). IL-4 acts as a myoblast recruitment factor during mammalian muscle growth. *Cell*, 113(4), 483-494.
29. Ieronimakis, N., Hays, A., Prasad, A., Janebodin, K., Duffield, J. S., & Reyes, M. (2016). PDGFR $\alpha$  signaling promotes fibrogenic responses in collagen-producing cells in Duchenne muscular dystrophy. *The Journal of Pathology*, 240(4), 410-424.
30. Ishikawa, Y., Miura, T., Ishikawa, Y., Aoyagi, T., Ogata, H., Hamada, S., & Minami, R. (2011). Duchenne muscular dystrophy: survival by cardio-respiratory interventions. *Neuromuscular Disorders*, 21(1), 47-51.
31. Isono, M., Chen, S., Hong, S. W., Iglesias-de la Cruz, M. C., & Ziyadeh, F. N. (2002). Smad pathway is activated in the diabetic mouse kidney and Smad3 mediates TGF- $\beta$ -induced fibronectin in mesangial cells. *Biochemical and Biophysical Research Communications*, 296(5), 1356-1365.
32. Ito, S., & Nagata, K. (2017). Biology of Hsp47 (Serpin H1), a collagen-specific molecular chaperone. In *Seminars in Cell & Developmental Biology*, 62, 142-15.
33. Jennekens, F.G., Ten Tate, L.P., De Visser, M., Wintzen, A.R. (1991) Diagnostic criteria for Duchenne and Becker muscular dystrophy and myotonic dystrophy. *Neuromuscular Disorders* 1(6), 389-391.

34. Kawai, H., Adachi, K., Nishida, Y., Inui, T., Kimura, C., & Saito, S. (1993). Decrease in urinary excretion of 3-methylhistidine by patients with Duchenne muscular dystrophy during glucocorticoid treatment. *Journal of Neurology*, *240*(3), 181-186.
35. Kazankov, K., Barrera, F., Møller, H. J., Bibby, B. M., Vilstrup, H., George, J., & Grønbaek, H. (2014). Soluble CD163, a macrophage activation marker, is independently associated with fibrosis in patients with chronic viral hepatitis B and C. *Hepatology*, *60*(2), 521-530.
36. Kim, J. M., Rasmussen, J. P., & Rudensky, A. Y. (2007). Regulatory T cells prevent catastrophic autoimmunity throughout the lifespan of mice. *Nature Immunology*, *8*(2), 191-197.
37. Kim, M. G., Kim, S. C., Ko, Y. S., Lee, H. Y., Jo, S. K., & Cho, W. (2015). The role of M2 macrophages in the progression of chronic kidney disease following acute kidney injury. *PLoS One*, *10*(12), e0143961.
38. Klingler, W., Jurkat-Rott, K., Lehmann-Horn, F., & Schleip, R. (2012). The role of fibrosis in Duchenne muscular dystrophy. *Acta Myologica*, *31*(3), 184.
39. Kliwinski, C., Kukral, D., Postelnek, J., Krishnan, B., Killar, L., Lewin, A., & Townsend, R. (2005). Prophylactic administration of abatacept prevents disease and bone destruction in a rat model of collagen-induced arthritis. *Journal of Autoimmunity*, *25*(3), 165-171.
40. Ko, H. J., Cho, M. L., Lee, S. Y., Oh, H. J., Heo, Y. J., Moon, Y. M., & Park, K. S. (2010). CTLA4-Ig modifies dendritic cells from mice with collagen-induced arthritis to increase the CD4<sup>+</sup> CD25<sup>+</sup> Foxp3<sup>+</sup> regulatory T cell population. *Journal of Autoimmunity*, *34*(2), 111-120.

41. Kuroda, K., & Tajima, S. (2004). HSP47 is a useful marker for skin fibroblasts in formalin-fixed, paraffin-embedded tissue specimens. *Journal of Cutaneous Pathology*, 31(3), 241-246.
42. Leitinger, N., & Schulman, I. G. (2013). Phenotypic polarization of macrophages in atherosclerosis. *Arteriosclerosis, Thrombosis, and Vascular biology*, 33(6), 1120-1126.
43. Lemos, D. R., Babaeijandaghi, F., Low, M., Chang, C. K., Lee, S. T., Fiore, D., & Rossi, F. M. (2015). Nilotinib reduces muscle fibrosis in chronic muscle injury by promoting TNF-mediated apoptosis of fibro/adipogenic progenitors. *Nature Medicine*, 21(7), 786-794.
44. Lenschow, D. J., Walunas, T. L., & Bluestone, J. A. (1996). CD28/B7 system of T cell costimulation. *Annual Review of Immunology*, 14(1), 233-258.
45. Liu, Y., Qingjuan, S., Gao, Z., Deng, C., Wang, Y., & Guo, C. (2017). Circulating fibrocytes are involved in inflammation and leukocyte trafficking in neonates with necrotizing enterocolitis. *Medicine*, 96(26).
46. Ma, J., Chen, T., Mandelin, J., Ceponis, A., Miller, N. E., Hukkanen, M., & Kontinen, Y. T. (2003). Regulation of macrophage activation. *Cellular and Molecular Life Sciences CMLS*, 60(11), 2334-2346.
47. McDouall, R. M., Dunn, M. J., & Dubowitz, V. (1990). Nature of the mononuclear infiltrate and the mechanism of muscle damage in juvenile dermatomyositis and Duchenne muscular dystrophy. *Journal of the Neurological Sciences*, 99(2-3), 199-217.
48. Merlini, L., Cicognani, A., Malaspina, E., Gennari, M., Gnudi, S., Talim, B., & Franzoni, E. (2003). Early prednisone treatment in Duchenne muscular dystrophy. *Muscle & Nerve*:

*Official Journal of the American Association of Electrodiagnostic Medicine*, 27(2), 222-227.

49. Mills, C. (2012). M1 and M2 macrophages: oracles of health and disease. *Critical Reviews in Immunology*, 32(6).
50. Mojumdar, K., Liang, F., Giordano, C., Lemaire, C., Danialou, G., Okazaki, T., & Petrof, B. J. (2014). Inflammatory monocytes promote progression of Duchenne muscular dystrophy and can be therapeutically targeted via CCR 2. *EMBO Molecular Medicine*, 6(11), 1476-1492.
51. Mosser, D. M., & Edwards, J. P. (2008). Exploring the full spectrum of macrophage activation. *Nature Reviews: Immunology*, 8(12), 958-969.
52. Najafian, N., & Sayegh, M. H. (2000). CTLA4-Ig: a novel immunosuppressive agent. *Expert Opinion on Investigational Drugs*, 9(9), 2147-2157.
53. Nawaz, A., Aminuddin, A., Kado, T., Takikawa, A., Yamamoto, S., Tsuneyama, K., & Takatsu, K. (2017). CD206+ M2-like macrophages regulate systemic glucose metabolism by inhibiting proliferation of adipocyte progenitors. *Nature Communications*, 8(1), 1-16.
54. Okada, H., Kajiya, H., Omata, Y., Matsumoto, T., Sato, Y., Kobayashi, T., & Sudo, S. (2019). CTLA4-Ig directly inhibits osteoclastogenesis by interfering with intracellular calcium oscillations in bone marrow macrophages. *Journal of Bone and Mineral Research*, 34(9), 1744-1752.
55. Pace, J.L., Russell, S.W., Schreiber, R.D., Altman, A., Katz, D.H. (1983) Macrophage activation: priming activity from a T-cell hybridoma is attributable to interferon-gamma. *Proceedings of the National Academy of Sciences of the United States of America* 80(12): 3782-2786.

56. Park, J. S., Gamboni-Robertson, F., He, Q., Svetkauskaite, D., Kim, J. Y., Strassheim, D., & Ishizaka, A. (2006). High mobility group box 1 protein interacts with multiple Toll-like receptors. *American Journal of Physiology-Cell Physiology*, 290(3), C917-C924.
57. Pechhold, K., Patterson, N. B., Craighead, N., Lee, K. P., June, C. H., & Harlan, D. M. (1997). Inflammatory cytokines IFN-gamma plus TNF-alpha induce regulated expression of CD80 (B7-1) but not CD86 (B7-2) on murine fibroblasts. *The Journal of Immunology*, 158(10), 4921-4929.
58. Petrof B.J., Shrager, J.B., Stedman, H.H., Kelly, A.M., Sweeney, H.L. (1993) Dystrophin protects the sarcolemma from stresses developed during muscle contraction. *Proceedings of the National Academy of Sciences of the United States of America*, 90, 3710-3714.
59. Philip, R. and Epstein, L.B. (1986) Tumour necrosis factor as immunomodulator and mediator of monocyte cytotoxicity induced by itself, gamma-interferon and interleukin-1. *Nature*, 323(6083), 86-89.
60. Ponsoye, M., Frantz, C., Ruzehaji, N., Nicco, C., Elhai, M., Ruiz, B., & Allanore, Y. (2016). Treatment with abatacept prevents experimental dermal fibrosis and induces regression of established inflammation-driven fibrosis. *Annals of the Rheumatic Diseases*, 75(12), 2142-2149.
61. Quattrocelli, M., Barefield, D. Y., Warner, J. L., Vo, A. H., Hadhazy, M., Earley, J. U., & McNally, E. M. (2017). Intermittent glucocorticoid steroid dosing enhances muscle repair without eliciting muscle atrophy. *The Journal of Clinical Investigation*, 127(6), 2418-2432.
62. Ruperto, N., Lovell, D. J., Quartier, P., Paz, E., Rubio-Pérez, N., Silva, C. A., & Saad-Magalhães, C. (2008). Abatacept in children with juvenile idiopathic arthritis: a

- randomised, double-blind, placebo-controlled withdrawal trial. *The Lancet*, 372(9636), 383-391.
63. Ruperto, N., Lovell, D. J., Quartier, P., Paz, E., Rubio-Pérez, N., Silva, C. A., & Saad-Magalhães, C. (2010). Long-term safety and efficacy of abatacept in children with juvenile idiopathic arthritis. *Arthritis & Rheumatism*, 62(6), 1792-1802.
64. Serra, F., Quarta, M., Canato, M., Toniolo, L., De Arcangelis, V., Trotta, A., & Naro, F. (2012). Inflammation in muscular dystrophy and the beneficial effects of non-steroidal anti-inflammatory drugs. *Muscle & Nerve*, 46(5), 773-784.
65. Shearer, J. D., Richards, J. R., Mills, C. D., & Caldwell, M. D. (1997). Differential regulation of macrophage arginine metabolism: a proposed role in wound healing. *American Journal of Physiology-Endocrinology and Metabolism*, 272(2), E181-E190.
66. Song, G., Yang, R., Zhang, Q., Chen, L., Huang, D., Zeng, J., & Zhang, T. (2019). TGF- $\beta$  secretion by M2 macrophages induces glial scar formation by activating astrocytes in vitro. *Journal of Molecular Neuroscience*, 69(2), 324-332.
67. Spencer, M. J., Walsh, C. M., Dorshkind, K. A., Rodriguez, E. M., & Tidball, J. G. (1997). Myonuclear apoptosis in dystrophic mdx muscle occurs by perforin-mediated cytotoxicity. *The Journal of Clinical Investigation*, 99(11), 2745-2751.
68. Spencer, M. J., Montecino-Rodriguez, E., Dorshkind, K., & Tidball, J. G. (2001). Helper (CD4+) and cytotoxic (CD8+) T cells promote the pathology of dystrophin-deficient muscle. *Clinical Immunology*, 98(2), 235-243.
69. Tonkin, J., Temmerman, L., Sampson, R. D., Gallego-Colon, E., Barberi, L., Bilbao, D., & Rosenthal, N. (2015). Monocyte/macrophage-derived IGF-1 orchestrates murine

skeletal muscle regeneration and modulates autocrine polarization. *Molecular Therapy*, 23(7), 1189-1200.

70. Tono, T., Aihara, S., Hoshiyama, T., Arinuma, Y., Nagai, T., & Hirohata, S. (2017). Effects of CTLA4-Ig on human monocytes. *Inflammation and Regeneration*, 37(1), 1-6.
71. Van Erp, C., Loch, D., Laws, N., Trebbin, A., & Hoey, A. J. (2010). Timeline of cardiac dystrophy in 3–18-month-old MDX mice. *Muscle & Nerve*, 42(4), 504-513.
72. Vidal, B., Serrano, A. L., Tjwa, M., Suelves, M., Ardite, E., De Mori, R., & Jardí, M. (2008). Fibrinogen drives dystrophic muscle fibrosis via a TGF $\beta$ /alternative macrophage activation pathway. *Genes & Development*, 22(13), 1747-1752.
73. Villalta, S. A., Nguyen, H. X., Deng, B., Gotoh, T., & Tidball, J. G. (2009). Shifts in macrophage phenotypes and macrophage competition for arginine metabolism affect the severity of muscle pathology in muscular dystrophy. *Human Molecular Genetics*, 18(3), 482-496.
74. Villalta, S. A., Deng, B., Rinaldi, C., Wehling-Henricks, M., & Tidball, J. G. (2011). IFN- $\gamma$  promotes muscle damage in the mdx mouse model of Duchenne muscular dystrophy by suppressing M2 macrophage activation and inhibiting muscle cell proliferation. *The Journal of Immunology*, 187(10), 5419-5428.
75. Villalta, S. A., Rinaldi, C., Deng, B., Liu, G., Fedor, B., & Tidball, J. G. (2011). Interleukin-10 reduces the pathology of mdx muscular dystrophy by deactivating M1 macrophages and modulating macrophage phenotype. *Human Molecular Genetics*, 20(4), 790-805.

76. Villalta, S. A., Rosenthal, W., Martinez, L., Kaur, A., Sparwasser, T., Tidball, J. G. & Bluestone, J. A. (2014). Regulatory T cells suppress muscle inflammation and injury in muscular dystrophy. *Science Translational Medicine*, 6(258), 258ra142-258ra142.
77. Wahl, S. M., Wahl, L. M., & McCarthy, J. B. (1978). Lymphocyte-mediated activation of fibroblast proliferation and collagen production. *The Journal of Immunology*, 121(3), 942-946.
78. Walcher, T., Steinbach, P., Spieß, J., Kunze, M., Gradinger, R., Walcher, D., & Bernhardt, P. (2011). Detection of long-term progression of myocardial fibrosis in Duchenne muscular dystrophy in an affected family: a cardiovascular magnetic resonance study. *European Journal of Radiology*, 80(1), 115-119.
79. Walunas, T. L., Bakker, C. Y., & Bluestone, J. A. (1996). CTLA-4 ligation blocks CD28-dependent T cell activation. *The Journal of Experimental Medicine*, 183(6), 2541-2550.
80. Walunas, T. L., Lenschow, D. J., Bakker, C. Y., Linsley, P. S., Freeman, G. J., Green, J. M., & Bluestone, J. A. (1994). CTLA-4 can function as a negative regulator of T cell activation. *Immunity*, 1(5), 405-413.
81. Warren, G. L., O'Farrell, L., Summan, M., Hulderman, T., Mishra, D., Luster, M. I., & Simeonova, P. P. (2004). Role of CC chemokines in skeletal muscle functional restoration after injury. *American Journal of Physiology-Cell Physiology*, 286(5), C1031-C1036.
82. Wehling, M., Spencer, M. J., & Tidball, J. G. (2001). A nitric oxide synthase transgene ameliorates muscular dystrophy in mdx mice. *The Journal of Cell Biology*, 155(1), 123-132.

83. Wehling-Henricks, M., Lee, J. J., & Tidball, J. G. (2004). Prednisolone decreases cellular adhesion molecules required for inflammatory cell infiltration in dystrophin-deficient skeletal muscle. *Neuromuscular Disorders*, *14*(8-9), 483-490.
84. Wehling-Henricks, M., Jordan, M. C., Gotoh, T., Grody, W. W., Roos, K. P., & Tidball, J. G. (2010). Arginine metabolism by macrophages promotes cardiac and muscle fibrosis in mdx muscular dystrophy. *PloS one*, *5*(5), e10763.
85. Wehling-Henricks, M., Welc, S. S., Samengo, G., Rinaldi, C., Lindsey, C., Wang, Y., & Tidball, J. G. (2018). Macrophages escape Klotho gene silencing in the mdx mouse model of Duchenne muscular dystrophy and promote muscle growth and increase satellite cell numbers through a Klotho-mediated pathway. *Human Molecular Genetics*, *27*(1), 14-29.
86. Welc, S. S., Flores, I., Wehling-Henricks, M., Ramos, J., Wang, Y., Bertoni, C., & Tidball, J. G. (2019). Targeting a therapeutic LIF transgene to muscle via the immune system ameliorates muscular dystrophy. *Nature communications*, *10*(1), 1-17.
87. Yılmaz, Ö., Karaduman, A., & Topaloğlu, H. (2004). Prednisolone therapy in Duchenne muscular dystrophy prolongs ambulation and prevents scoliosis. *European Journal of Neurology*, *11*(8), 541-544.
88. Zhu, L., Fu, X., Chen, X., Han, X., & Dong, P. (2017). M2 macrophages induce EMT through the TGF- $\beta$ /Smad2 signaling pathway. *Cell Biology International*, *41*(9), 960-968